Available online at www.sciencedirect.com
SCIENCE DIRECT®
Journal of Computational Physics 202 (2005) 411–445
JOURNAL OF COMPUTATIONAL PHYSICS
www.elsevier.com/locate/jcp

A numerical method for solving variable coefficient elliptic equation with interfaces ☆

Songming Hou, Xu-Dong Liu *

Department of Mathematics, University of California Santa Barbara, Santa Barbara, CA 93106, USA

Received 9 July 2003; received in revised form 14 July 2004; accepted 14 July 2004
Available online 1 October 2004

Abstract

A new 2nd order accurate numerical method on non-body-fitting grids is proposed for solving the variable coefficient elliptic equation in disjoint subdomains $\Omega^{\pm}$ separated by interfaces Γ. The variable coefficients, the source term, and hence the solution itself and its derivatives may be discontinuous across the interfaces. Jump conditions in solution and its co-normal derivative at interface are prescribed. Instead of smooth, the interfaces are only required to be Lipschitz continuous as submanifold. A weak formulation is developed, the existence, uniqueness and regularity of the solutions are studied. The numerical method is derived by discretizing the weak formulation. The method is different from traditional finite element methods. Extensive numerical experiments are presented and show that the method is 2nd order accurate in solution and 1st order accurate in its gradient in L^{∞} norm if the interface is C^2 and solutions are C^2 on the closures of the subdomains. The method can handle the problems when the solutions and/or the interfaces are weaker than C^2. For example, $u \in H^2(\Omega^{\pm})$, Γ is Lipschitz continuous and their singularities coincide, see Example 18 in Section 4. The accuracies of the method under various circumstances are listed in Table 19.

MSC: 65N30; 35J25
Keywords: Elliptic equation; Non-smooth interface; Jump conditions; Weak formulation

1. Introduction

The "immersed boundary" method [13,14] uses a numerical approximation of δ-function which smears out the solution on a thin finite band around the interface Γ. In [15], the "immersed boundary" method was

☆ Research partially supported by the National Science Foundation: DMS-0107419.
* Corresponding author.
E-mail address: xliu@math.ucsb.edu (X.-D. Liu).

0021-9991/$ - see front matter © 2004 Elsevier Inc. All rights reserved.
doi:10.1016/j.jcp.2004.07.016

combined with the level set method resulting in a first order numerical method that is simple to implement even in multiple spatial dimensions. However, for both methods, the numerical smearing at the interface forces continuity in solution at the interface regardless of the interface condition $[u] = a$, where a might not be zero.

In [10,11], a fast method for solving Laplace's equations on irregular regions with smooth boundaries was introduced. By using Fredholm integral equation of the second kind, solutions can be extended to a rectangular region. Since solutions are harmonic, Fredholm integral equations can be used again to capture the jump conditions in solution and its normal derivative, $[u] \neq 0$ and $[u_n] = 0$. Then these jump conditions are used to evaluate discrete Laplacian, and then fast Poisson solver on a regular region can be applied with 2nd or higher order accuracy.

In [5], the ''immersed interface'' method was presented. The method achieves a second order accuracy by incorporating the interface conditions into the finite difference stencil in a way that preserves the interface conditions in both solution and its co-normal derivative, $[u] \neq 0$ and $[\beta u_n] \neq 0$. The corresponding linear system is sparse but not symmetric or positive definite. A fast iterative method [6] conjuncted with ''immersed interface'' method has been developed for constant coefficient problems with interface conditions, and achieves 2nd order accuracy.

In [1], a finite element method was developed for solving such a problem with the interface conditions $[u] = 0$ and $[\beta u_n] \neq 0$. Interfaces are aligned with cell boundaries. The 2nd order accuracy was obtained in an energy norm. Nearly the 2nd order of accuracy was obtained in L^2 norm.

In [7], another finite element method was developed for solving the problem with the interface conditions $[u] = 0$ and $[\beta u_n] \neq 0$. Non-body-fitting Cartesian grids are used, and then associated uniform triangulations are added on. Interfaces are not necessarily aligned with cell boundaries. Numerical evidence shows that its conforming version achieves 2nd order accuracy in L^∞ norm, and higher than first order for its non-conforming version.

The boundary condition capturing method [8] uses the Ghost fluid method (GFM) [2] to capture the boundary conditions. The GFM is robust and simple to implement, so is the resulting boundary condition capturing method. The boundary condition capturing method is implemented using a standard finite difference discretization on a non-body-fitting Cartesian grid, making it simple to apply in multi-dimensions, including three spatial dimensions. Furthermore, the coefficient matrix of the associated linear system is the standard symmetric positive definite matrix for the variable coefficient Poisson equation in the absence of interfaces allowing for straightforward application of standard ''black box'' solvers. The boundary condition capturing method has been speeded up by a multi-grid method [16]. The convergence proof of the method is provided in [9]. In [9], a weak formulation of the problem was studied. The boundary condition capturing method can be obtained from discretizing the weak formulation. The convergence proof follows naturally. The boundary condition capturing method can solve the elliptic equation with interface conditions $[u] \neq 0$ and $[\beta u_n] \neq 0$ in multi-dimensions (including 2 dimensions and 3 dimensions), however the boundary condition capturing method is only first order accurate. For a similar problem, a Poisson equation with Dirichlet interface conditions (instead of jump conditions) on the irregular interface, the boundary condition capturing method is extended [3] by Gibou and Fedkiw, etc. (by using GFM [2]) to 2nd order accuracy in L^∞ and L^2 norms. The resulting linear system of the 2nd order accurate method is symmetric, which can readily be inverted with a number of fast methods.

In this paper, inspired by the boundary condition capturing method [8] and the weak formulation derived in [9]. The weak formulation is extended to include the case that the boundary and the subdomains' boundaries are only required to be Lipschitz continuous as submanifold. A numerical method is proposed by discretizing the weak formulation on a non-body-fitting grid. The method is capable of solving the elliptic equation with variable coefficients and non-homogeneous interface conditions $[u] \neq 0$ and $[\beta u_n] \neq 0$, and is capable of dealing with the case that the boundary and the subdomains' boundaries are only Lipschitz continuous. Extensive numerical experiments are presented and show that the method is 2nd order accurate

in solution and 1st order accurate in its gradients in L^∞ norm if the interface is C^2 and solutions are C^2 on the closures of the subdomains. The method can handle the problems when the solutions and/or the interfaces are weaker than C^2. For example, $u \in H^2(\Omega^\pm)$, Γ is Lipschitz continuous and their singularities coincide, see Example 18 in Section 4. The accuracies of the method under various circumstances are listed in Table 19.

2. Equations and weak formulation

Consider an open bounded domain $\Omega \subset \mathbb{R}^d$. Let Γ be an interface of co-dimension $d-1$, which divides Ω into disjoint open subdomains, Ω^- and Ω^+, hence $\Omega = \Omega^- \cup \Omega^+ \cup \Gamma$. Assume that the boundary $\partial\Omega$ and the boundary of each subdomain $\partial\Omega^\pm$ are Lipschitz continuous as submanifold. Since $\partial\Omega^\pm$ are Lipschitz continuous, so is Γ. A unit normal vector of Γ can be defined a.e. on Γ and points from Ω^- to Ω^+, see Section 1.5 in [4].

We seek solutions of the variable coefficient elliptic equation away from the interface Γ given by

$$\nabla \cdot (\beta(x)\nabla u(x)) = f(x), \quad x \in \Omega \setminus \Gamma, \tag{2.1a}$$

in which $x = (x_1, \ldots, x_d)$ denotes the spatial variables and ∇ is the gradient operator. The coefficient $\beta(x)$ is assumed to be a symmetric, uniformly elliptic and bounded $d \times d$ matrix, the components of which are continuously differentiable on the closure of each disjoint subdomain, Ω^- and Ω^+, but they may be discontinuous across the interface Γ. The uniformly ellipticity and boundedness of $\beta(x)$ is in the sense that there are two positive constants $0 < m \leqslant M < +\infty$ such that $m\mathbf{I} \leqslant \beta(x) \leqslant M\mathbf{I}$ for $\forall x \in \Omega$, where $\mathbf{I}$ stands for the $d \times d$ identity matrix. The right-hand side $f(x)$ is assumed to lie in $L^2(\Omega)$.

Given functions a and b along the interface Γ, we prescribe the jump conditions

$$\begin{cases} [u]_\Gamma(x) \equiv u^+(x) - u^-(x) = a(x), \\ \left[(\beta u)_n\right]_\Gamma(x) \equiv (\beta u)_n^+(x) - (\beta u)_n^-(x) = b(x), \end{cases} \quad x \in \Gamma, \tag{2.1b}$$

with the notation $(\beta u)_n = n \cdot \beta \nabla u$. The "$\pm$" superscripts refer to limits taken from within the subdomains $\Omega^\pm$.

Finally, we prescribe boundary conditions

$$u(x) = g(x), \quad x \in \partial\Omega \tag{2.1c}$$

for a given function g on the boundary $\partial\Omega$.

In [9], a weak formulation of the problem has been obtained in the case that the boundary $\partial\Omega$ and the interface Γ are smooth, and the interface Γ does not intersect with the boundary $\partial\Omega$. Here we extend the weak formulation a bit to include the case that the boundary $\partial\Omega$ and subdomains' boundaries $\partial\Omega^\pm$ are only Lipschitz continuous instead of smooth, and the interface Γ is allowed to intersect with the boundary $\partial\Omega$.

We are going to use the usual Sobolev spaces $H_0^1(\Omega)$ and $H^1(\Omega)$. We use the usual inner product for $H^1(\Omega)$. For $H_0^1(\Omega)$, instead of the usual inner product we choose one which is better suited to our problem:

$$B[u, v] = \int_{\Omega^+} \beta \nabla u \cdot \nabla v + \int_{\Omega^-} \beta \nabla u \cdot \nabla v. \tag{2.2}$$

This induces a norm on $H_0^1(\Omega)$ which is equivalent to the usual one, thanks to the Poincaré inequality and the uniformly ellipticity and boundedness of $\beta(x)$ on Ω.

Let be any closed Lipschitz continuous hyper-surface of dimension $d-1$ in $\overline{\Omega}$, where the overline denotes the closure of a set. Let R denote the restriction operator from $H^1(\Omega)$ to $L^2()$. This restriction operator R is well defined and is a bounded map, because is closed Lipschitz continuous (see Theorem 2.4.2 in [12])

and $C^1(\overline{\Omega})$ is dense in $H^1(\Omega)$. Throughout this section, we shall always assume that our interface data a and b are the restrictions of functions $\tilde{a}$ and $\tilde{b} \in H^1(\Omega)$ on $\partial\Omega^-$ and then limited on Γ, respectively. That is on Γ,

$$a = R_{\partial\Omega^-}(\tilde{a}) \quad \text{and} \quad b = R_{\partial\Omega^-}(\tilde{b}). \tag{2.3}$$

We shall always assume that our boundary data g can be obtained by the following way: Assume that there exist a function $\tilde{c} \in H^1(\Omega)$ and g is given as, on $\partial\Omega$,

$$g = \begin{cases} R_{\partial\Omega}(\tilde{c} - \tilde{a}), & \text{on } \partial\Omega \cap \partial\Omega^-, \\ R_{\partial\Omega}(\tilde{c}), & \text{on } \partial\Omega \setminus \partial\Omega^-. \end{cases} \tag{2.4}$$

This (2.4) could be thought as a compatibility condition between a and g. To simplify the notation, from now on we will drop the tildes.

We will construct a unique solution of the problem in the class

$$H(a,c) = \{u : u - c + a\chi(\overline{\Omega^-}) \in H_0^1(\Omega)\}. \tag{2.5}$$

If $u \in H(a,c)$, then $[u]_\Gamma = a$ and $u|_{\partial\Omega} = g$. Note that $H_0^1(\Omega)$ can be identified with $H(0,0)$.

Definition 2.1. A function $u \in H(a,c)$ is a weak solution of (2.1a)–(2.1c), if $v = u - c + a\chi(\overline{\Omega^-}) \in H_0^1(\Omega)$ satisfies

$$-B[v,\psi] = F(\psi) \tag{2.6a}$$

for all $\psi \in H_0^1(\Omega)$, where

$$\begin{aligned} B[v,\psi] &= \int_{\Omega^+} \beta\nabla v \cdot \nabla\psi + \int_{\Omega^-} \beta\nabla v \cdot \nabla\psi \quad \text{and} \\ F(\psi) &= \int_\Omega f\psi + \int_\Omega \beta\nabla c \cdot \nabla\psi - \int_{\Omega^-} \beta\nabla a \cdot \nabla\psi + \int_\Gamma b\psi. \end{aligned} \tag{2.6b}$$

Or equivalently

Definition 2.2. A function $u \in H(a,c)$ is a weak solution of (2.1a)–(2.1c), if u satisfies, for all $\psi \in H_0^1(\Omega)$,

$$-\left(\int_{\Omega^+} \beta\nabla u \cdot \nabla\psi + \int_{\Omega^-} \beta\nabla u \cdot \nabla\psi\right) = \int_\Omega f\psi + \int_\Gamma b\psi. \tag{2.7}$$

A classical solution of (2.1a)–(2.1c), $u|_{\Omega^\pm} \in C^2(\overline{\Omega^\pm})$, is necessarily a weak solution. Because all the subdomains' boundaries $\partial\Omega^\pm$ are Lipschitz continuous, the integration by parts are legal in each subdomain, $\Omega^\pm$, see Theorem 1.5.3.1 in [4].

Theorem 2.1. *If $f \in L^2(\Omega)$, and a, b, and $c \in H^1(\Omega)$, then there exists a unique weak solution of (2.6a) and (2.6b) in $H(a,c)$.*

Proof. The left-hand side (2.6b) of (2.6a) is a symmetric, bounded and elliptic bilinear form on $H_0^1(\Omega)$. The boundedness and the ellipticity are ensured by the fact that $\beta(x)$ is a symmetric, uniformly elliptic and bounded matrix in Ω. It is straightforward to see that the first three terms of $F(\psi)$ in (2.6b) are bounded linear functionals on $H_0^1(\Omega)$. Since $\psi = 0$ on $\partial\Omega$, the last term of $F(\psi)$ in (2.6b) $\int_\Gamma b\psi = \int_{\partial\Omega^-} b\psi$. Because of the boundedness of the restriction map $R_{\partial\Omega^-}$, the last term of $F(\psi)$ in (2.6b), $\int_\Gamma b\psi$, is a bounded linear functional on $H_0^1(\Omega)$, so is the $F(\psi)$ (2.6b) of (2.6a). By the Lax–Milgram Lemma, there exists a unique $v \in H_0^1(\Omega)$ (so a unique weak solution $u = v + c - a\chi(\overline{\Omega^-}) \in H(a,c)$) such that $-B[v,\psi] = F(\psi)$, for all $\psi \in H_0^1(\Omega)$.

Remark 1. a, b and c are assume to be $H^1(\Omega)$. The solution u is independent of the values of a and b away from Γ, and the values of c away from $\partial\Omega$. Assume there are two sets of data $\{a_1,b_1,c_1\}$ and $\{a_2,b_2,c_2\}$, and they match in the following way: $a_1 = a_2$ and $b_1 = b_2$ on Γ, and $-c_1 + a_1\chi(\overline{\Omega^-}) = -c_2 + a_2\chi(\overline{\Omega^-}) = -g$ on $\partial\Omega$. Let $u_1 = v_1 + c_1 - a_1\chi(\overline{\Omega^-})$ and $u_2 = v_2 + c_2 - a_2\chi(\overline{\Omega^-})$ be two weak solutions corresponding to $\{a_1,b_1,c_1\}$ and $\{a_2,b_2,c_2\}$, respectively, where $v_1, v_2 \in H_0^1(\Omega)$. $(a_2 - a_1)\chi(\overline{\Omega^-})$ is a H^1 function in Ω^-, $a_2 - a_1 = 0$ on Γ, and $(a_2 - a_1)\chi(\overline{\Omega^-}) = 0$ on $\Gamma \cup \Omega^+$. Since the boundary $\partial\Omega$ and the subdomains' boundaries $\partial\Omega^{\pm}$ are Lipschitz continuous, $(a_2 - a_1)\chi(\overline{\Omega^-})$ is a H^1 function in Ω. Thus $u_1 - u_2 = (v_1 - v_2) + (c_1 - c_2) - (a_1 - a_2)\chi(\overline{\Omega^-})$ is a H^1 function in Ω. Since $u_1 = u_2 = g$ on $\partial\Omega$, $u_1 - u_2 \in H_0^1(\Omega)$. It is easy to see that $u_1 - u_2 \in H_0^1(\Omega)$ satisfies $-\int_{\Omega^-}\beta\nabla(u_1 - u_2)\cdot\nabla\psi - \int_{\Omega^+}\beta\nabla(u_1 - u_2)\cdot\nabla\psi = 0$, for any $\psi \in H_0^1(\Omega)$. Therefore $u_1 = u_2$.

3. Numerical method

For ease of discussion in this section, and accuracy testing in the next section, we assume that a, b and c are smooth on the closure of Ω. We also assume that β and f are smooth on the closure of each Ω^+ and Ω^-, but they may be discontinuous across the interface Γ. However $\partial\Omega$, $\partial\Omega^-$ and $\partial\Omega^+$ are kept to be Lipschitz continuous. We assume that there is a Lipschitz continuous and piecewise smooth level-set function on $\overline{\Omega}$, which $\Gamma = \{\phi = 0\}$, $\Omega^- = \{\phi < 0\}$ and $\Omega^+ = \{\phi > 0\}$. A unit vector $n = \frac{\nabla\phi}{|\nabla\phi|}$ can be obtained on $\overline{\Omega}$, which is a unit normal vector of Γ at Γ pointing from Ω^- to Ω^+.

3.1. Grid and interpolation

For simplicity, in this paper, we restrict ourselves to the special case of a rectangular domain $\Omega = (x_{\min}, x_{\max}) \times (y_{\min},y_{\max})$ in the plane, and β is scalar. Given positive integers I and J, set $\Delta x = (x_{\max} - x_{\min})/I$ and $\Delta y = (y_{\max} - y_{\min})/J$. We define a uniform Cartesian grid $\{(x_i,y_j)\} = \{(x_{\min} + i\Delta x, y_{\min} + j\Delta y)\}$ for $i = 0, \ldots, I$ and $j = 0, \ldots, J$. Each (x_i,y_j) is called a grid point. A grid point is called a boundary point if $i = 0, I$ or $j = 0, J$; otherwise an interior point. The grid size is defined as $h = \max(\Delta x,\Delta y) > 0$.

Two sets of grid functions are needed and denoted by

$$H^{1,h} = \{\omega^h = (\omega_{i,j}) : \ 0 \leqslant i \leqslant I, 0 \leqslant j \leqslant J\}, \quad \text{and} \tag{3.1a}$$

$$H_0^{1,h} = \{\omega^h = (\omega_{i,j}) \in H^{1,h} : \ \omega_{i,j} = 0 \text{ if } i = 0, I \text{ or } j = 0, J\}. \tag{3.1b}$$

For each rectangular region $[x_i,x_{i+1}] \times [y_j,y_{j+1}]$, we cut it into two pieces of right triangular regions: one is bounded by $x = x_i$, $y = y_j$ and $y = \frac{y_{j+1}-y_j}{x_i - x_{i+1}}(x - x_{i+1}) + y_j$, and the other is bounded by $x = x_{i+1}$, $y = y_{j+1}$ and $y = \frac{y_{j+1}-y_j}{x_i - x_{i+1}}(x - x_{i+1}) + y_j$. Collect all those triangular regions, we obtain a uniform triangulation $\mathbf{T}^h$: $\overline{\Omega} = \bigcup_{K\in\mathbf{T}^h} K$. See Fig. 1. We can also choose the hypotenuse to be $y = \frac{y_{j+1}-y_j}{x_{i+1}-x_i}(x - x_i) + y_j$, and get another uniform triangulation from the same Cartesian grid. There is no conceptual difference of our method on these two triangulations.

If $\phi(x_i,y_j) \leqslant 0$, we count the grid point (x_i,y_j) as in $\overline{\Omega^-}$; otherwise in Ω^+. We call an edge (an edge of a triangle in the triangulation) an interface edge if two of its ends (vertexes of triangles in the triangulation) belong to different subdomains; or otherwise a regular edge.

We call a cell K an interface cell if its vertices's belong to different subdomains, and clearly the interface goes through the interface cell K. In the interface cell, we write $K = K^+ \cup K^-$. K^+ and K^- are separated by a straight line segment, denoted by Γ_K^h. Two end points of the line segment Γ_K^h are located on the interface Γ and their locations can be calculated by the linear interpolations of the discrete level-set functions $\phi^h = \{\phi(x_i,y_j)\}$. The vertices's of K^+ are located in $\Omega^+ \cup \Gamma$ and the vertexes of K^- are located in $\Omega^- \cup \Gamma$. K^+ and K^-

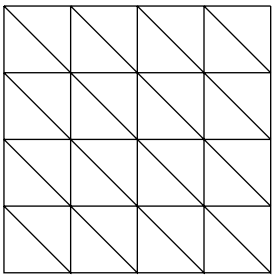

Fig. 1. A uniform triangulation.

are approximations of the regions of $K \cap \Omega^+$ and $K \cap \Omega^-$, respectively. We call a cell K a regular cell if all its vertexes belong to the same subdomain, either Ω^+ or Ω^-. For a regular cell, we also write $K = K^+ \cup K^-$, where $K^- = \{\}$ (empty set) if all vertexes of K are in Ω^+, and $K^+ = \{\}$ (empty set) if all vertexes of K are in Ω^-. Clearly $\Gamma_K^h = \{\}$(empty set) in a regular cell, and K^+ and K^- are approximations of the regions $K \cap \Omega^+$ and $K \cap \Omega^-$, respectively. We use $|K^+|$ and $|K^-|$ to represent the areas of K^+ and K^-, respectively.

Remark 2. The Γ_K^h is a good approximation of $\Gamma \cap K$ for the C^1 or smoother interfaces, see Examples 1–6, 10–15. The Γ_K^h is not a good approximation of $\Gamma \cap K$ for the Lipschitz continuous interfaces in general, see Examples 7, 8, 16, 17, and 18, unless all kinks are on the edges of triangles of the triangulation, see Example 9.

Two extension operators are needed. The first one is $T^h : H_0^{1,h} \rightarrow H_0^1(\Omega)$. For any $\psi^h \in H_0^{1,h}$, $T^h(\psi^h)$ is a standard continuous piecewise linear function, which is a linear function in every triangular cell and $T^h(\psi^h)$ matches ψ^h on grid points. Clearly such function set, denoted by $\overline{H_0^{1,h}}$, is a finite dimensional subspace of $H_0^1(\Omega)$.

The second extension operator U^h is constructed as follows. For any $u^h \in H^{1,h}$ with $u^h = g^h$ at boundary points, $U^h(u^h)$ is a piecewise linear function and matches u^h on grid points. It is a linear function in each regular cell, just like the first extension operator $U^h(u^h) = T^h(u^h)$ in regular cell. In each interface cell, it consists of two pieces of linear functions, one is on K^+ and the other is on K^-. The location of its discontinuity in the interface cell is the straight line segment Γ_K^h. Note that two end points of the line segment are located on the interface Γ, and hence the interface condition $[u] = a$ could be and is enforced exactly at these two end points. In each interface cell, the interface condition $[\beta \nabla u \cdot n] = b$ is enforced with the value b at the middle point of Γ_K^h. Clearly such a function is not continuous in general, neither the set of such functions a linear space. We denote the set of such functions as $\overline{H_{a,c}^{1,h}}$, which should be thought as an approximation of the solution class $H(a,c)$ (2.5) plus the restriction of $[\beta u_n] = b$. Similar versions of such extension can be found in the literature [7,8]. In order to use this extension, we need the following lemma.

Lemma 6.1. *$\forall u^h \in H^{1,h}$, $U^h(u^h)$ can be constructed uniquely, provided $\mathbf{T}^h$, ϕ, a and b are given (The proof is provided in Appendix A).*

Since linear interpolations are used in approximating interfaces and solutions, the order of accuracy of the method is expected to be 2nd order in some norm or, the "best" hopeful, the 2nd order in L^∞ norm.

3.2. Discrete weak formulation

Under the current setting, we discretize the weak formulation (2.7) as follows:

Method 3.1. Find a discrete function $u^h \in H^{1,h}$ such that

$$u^h = g^h \quad \text{on boundary points} \tag{3.2a}$$

and for all $\psi^h \in H_0^{1,h}$,

$$-\sum_{K\in\mathbf{T}^h}\left(\int_{K^+}\beta\nabla U^h(u^h)\cdot\nabla T^h(\psi^h)+\int_{K^-}\beta\nabla U^h(u^h)\cdot\nabla T^h(\psi^h)\right)$$
$$=\sum_{K\in\mathbf{T}^h}\left(\int_{K^+}fT^h(\psi^h)+\int_{K^-}fT^h(\psi^h)+\int_{\Gamma_K^h}bT^h(\psi^h)\right). \tag{3.2b}$$

Note that $u = g$ on the boundary is the same as $u - c + a\chi(\overline{\omega^-}) = 0$ on the boundary.

Remark 3. Our method uses weak formulations, as finite element methods do. However the solution set $\overline{H_{a,c}^{1,h}}$ is not a linear space, which is different from traditional finite element methods.

$H_0^{1,h}$ is a finite dimensional linear space and its dimension is the number of interior grid points. We construct its base as follows. For $m = 1,\ldots,I-1$ and $n = 1,\ldots,J-1$, let $\psi_{m,n}^h = \{\delta_{i,m}\delta_{j,n} : i = 0,\ldots,I, j = 0,\ldots,J\} \in H_0^{1,h}$ where $\delta_{i,m} = 1$, if $i = m$ and $\delta_{i,\,m} = 0$, if $i \neq m$. Hence our Method 3.1 can be rewritten as

Method 3.2. Find a discrete function $u^h = \{u_{i,j}\} \in H^{1,h}$ such that

$$u^h = g^h \quad \text{on the boundary points} \tag{3.3a}$$

and for every discrete base function $\psi_{m,n}^h$ of $H_0^{1,h}$,

$$-\sum_{K\in\mathbf{T}^h}\left(\int_{K^+}\beta\nabla U^h(u^h)\cdot\nabla T^h(\psi_{m,n}^h)+\int_{K^-}\beta\nabla U^h(u^h)\cdot\nabla T^h(\psi_{m,n}^h)\right)$$
$$=\sum_{K\in\mathbf{T}^h}\left(\int_{K^+}fT^h(\psi_{m,n}^h)+\int_{K^-}fT^h(\psi_{m,n}^h)+\int_{\Gamma_K^h}bT^h(\psi_{m,n}^h)\right). \tag{3.3b}$$

Remark 4. Let $\mathbf{T}^h$ be any irregular "triangulations" in multi-dimensions. Let $H^{1,h}$ and $H_0^{1,h}$ be proper grid function spaces in multi-dimensions. Let U^h and T^h be corresponding extensions in multi-dimensions. Method 3.2 also works on irregular "triangulations" in any space dimensions. Uniform "triangulations", which result from uniform Cartesian grids, are simpler and less expensive compared to irregular "triangulations". Since the method uses non-body-fitting grids and captures discontinuities at interfaces so well (2nd order accurate in L^∞ norm), the expected disadvantage in resolutions at and near interfaces of non-body-fitting uniform "triangulations" compared to body-fitting irregular "triangulations" is significantly reduced. Therefore we propose the method using non-body-fitting irregular "triangulations" and uniform "triangulations", so that potential users can have their choices.

Remark 5. Because the method uses non-body-fitting "triangulations", the method could use irregular "triangulations" or uniform "triangulations". For methods using body-fitting "triangulations", irregular "triangulations" are required and uniform "triangulations" can not be used in general. Method using body-fitting grids have another drawback. If the interfaces move, costly grid regenerations are required as time goes.

Remark 6. The method proposed here is independent of the values of c away from $\partial\Omega$ or the values of a away from Γ. It does depend on the values of b near Γ, because Γ_K^h approximates and in general is not equal to $\Gamma \cap K$. So do the numerical solutions. However the weak solution is independent of the values of b away from Γ and the numerical solutions converge to the weak solution. Extensive numerical experiments are

presented and show that the method is 2nd order accurate in solution and 1st order accurate in its gradients in L^∞ norm if the interface is C^2 and solutions are C^2 on the closures of subdomains. The method can handle the problems when the solutions and/or the interfaces are weaker than C^2. For example, $u \in H^2(\Omega^\pm)$, Γ is Lipschitz continuous and their singularities coincide, see Example 18 in Section 4. The accuracies of the method under various circumstances are listed in Table 19. Therefore the dependence of the numerical solutions on the data is acceptable. Potential readers and/or users could try to find optimal data b, which is beyond the scope of this paper.

4. Numerical experiments

Consider the problem

$$\begin{cases} \nabla \cdot (\beta \nabla u) = f, & \text{in } \Omega^\pm, \\ [u] = a, & \text{on } \Gamma, \\ [\beta u_n] = b, & \text{on } \Gamma, \\ u = g, & \text{on } \partial\Omega, \end{cases}$$

on the rectangular domain $\Omega = (x_{\min},x_{\max}) \times (y_{\min},y_{\max})$. Γ is an interface and prescribed by the zero level-set $\{(x,y) \in \Omega | \phi(x,y) = 0\}$ of a level-set function $\phi(x,y)$. The unit normal vector of Γ is $n = \frac{\nabla\phi}{|\nabla\phi|}$ pointing from $\Omega^- = \{(x,y) \in \Omega | \phi(x,y) \leqslant 0\}$ to $\Omega^+ = \{(x,y) \in \Omega | \phi(x,y) \rangle\}$.

In all numerical experiments below, the level-set function $\phi(x,y)$, the coefficients $\beta^\pm(x,y)$ and the solutions

$$(u(x,y) = \begin{cases} u^+(x,y), & \Omega^+, \\ u^-(x,y), & \Omega^- \end{cases}$$

are given. Hence $f = \nabla \cdot (\beta \nabla u)$, $a = u^+ - u^-$ and $b = \beta^+ u_n^+ - \beta^- u_n^-$ can be derived on the whole domain Ω. g is obtained by the proper Dirichlet boundary condition, since the solutions are given.

Sequences of uniform Cartesian grids are used $\Omega^k = \{(x_i,y_j) | x_i = x_{\min} + i\,\mathrm{d}x^k,\ \ y_j = y_{\min} + j\,\mathrm{d}y^k, i = 0, \ldots, I^k, j = 0, \ldots, J^k\}$. $\mathrm{d}x^k = (x_{\max} - x_{\min})/I^k$ is the step-size in x direction and $I^k + 1$ is the number of grid points in x direction. $\mathrm{d}y^k = (y_{\max} - y_{\min})/J^k$ is the step-size in y direction and $J^k + 1$ is the number of grid points in y direction.

The interface might hit grid points, which may cause inaccuracy in dealing with a situation of zero over zero. To avoid this, set $\phi(x_i,y_j) = -\epsilon$, if $|\phi(x_i,y_j)| < \epsilon$ ($=10^{-8}\Delta x$ in all calculations). For simplicity reason, in each triangular cell K, set β^+ to be the β value at the center of K^+, and β^- the β value at the center of K^-. They approximate $\frac{1}{|K^+|}\int_{K^+}\beta$ and $\frac{1}{|K^-|}\int_{K^-}\beta$ within enough accuracy. To evaluate $\int_{K^+} fT^h(\psi^h_{mn})$, first cut K^+ into two triangles if K^+ is not a triangle, then on each triangle, use a 2nd order accurate numerical quadrature. Evaluate $\int_{K^-} fT^h(\psi^h_{mn})$ similarly. Use the 2nd order accurate midpoint rule to evaluate $\int_{\Gamma^h_K} bT^h(\psi^h_{mn})$.

All errors in solutions are measured in L^∞ norm in the whole domain Ω. All errors in gradient of solutions are measured in L^∞ norm away from interfaces.

4.1. Smooth interfaces and smooth solutions

In all experiments of this subsection, all interfaces are C^∞, all solutions are $C^\infty(\overline{\Omega^\pm})$ and the domains are $(-1,1) \times (-1,1)$. Two different sequences of grids are used to check if the method is insensitive to the grids. All experiments in this subsection show that the method is insensitive to the grids if the interfaces and solutions are smooth.

Example 1. The level-set functions ϕ, the coefficients $\beta^{\pm}$ and the solution $u^{\pm}$ are given as follows:

$$\phi_1 = x^2 + y^2 - 0.25 \quad \text{or} \quad \phi_2 = \sqrt{x^2 + y^2} - 0.5,$$
$$\beta^+ = \sin(x + y) + 2, \quad \beta^- = \cos(x + y) + 2,$$
$$u^+ = \ln(x^2 + y^2), \quad u^- = \sin(x + y).$$

Fig. 2 shows the numerical solution of the method using 321 number of points in both x and y directions. Upper (with $\phi = \phi_1 = x^2 + y^2 - 0.25$) and lower (with $\phi = \phi_2 = \sqrt{x^2 + y^2} - 0.5$) halves of the Table 1 shows that the method achieves 2nd order accuracy in solutions and first order accuracy in its gradients on two different sets of grids. The method is not sensitive to (1) the forms of level-set functions or (2) the grids.

Example 2. The level-set function ϕ, the coefficients $\beta^{\pm}$ and the solution $u^{\pm}$ are given as follows:

$$\phi = x^2 + y^2 - 0.25,$$
$$\beta^+ = x^2 - y^2 + 3, \quad \beta^- = 1000(xy + 3),$$
$$u^+ = 1 - x^2 - y^2, \quad u^- = x^2 + y^2 + 2.$$

Fig. 3 shows the numerical solution of the method using 321 number of points in both x and y directions. The difficulty of the example is that $\beta^+/\beta^- \approx 1/1000$. Table 2 shows that the method achieves 2nd order accuracy in solutions and first order accuracy in its gradient on two different sets of grids. The method is not sensitive to the grids.

Example 3. The level-set function ϕ, the coefficients $\beta^{\pm}$ and the solution $u^{\pm}$ are given as follows:

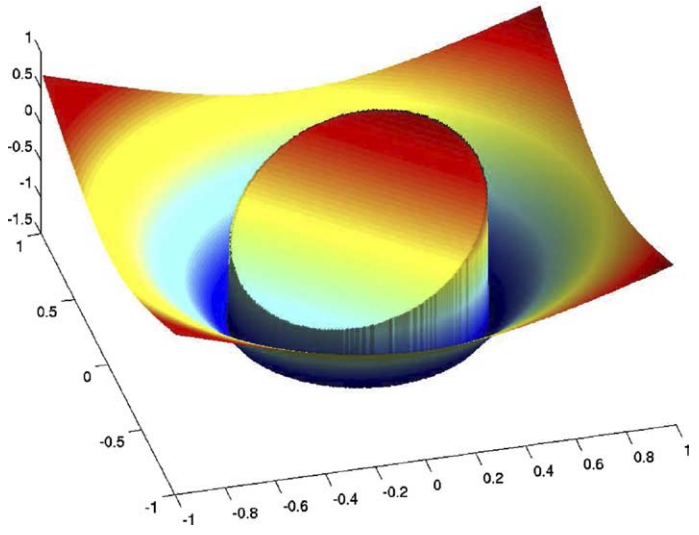

Fig. 2. The method is NOT sensitive to the forms of level-set functions or grids.

Table 1
Upper half for $\phi = \phi_1 = x^2 + y^2 - 0.25$ and lower half for $\phi = \phi_2 = \sqrt{x^2 + y^2} - 0.5$

ϕ	# of pts in x, y	Err in U	Order	Err in ∇U	Order
$\phi = \phi_1$	40, 40	2.30e−3		1.39e−2	
	80, 80	5.54e−4	2.06	5.85e−3	1.25
	160, 160	1.36e−4	2.02	2.22e−3	1.40
	320, 320	3.64e−5	1.90	1.00e−3	1.14
	41, 39	2.28e−3		1.40e−2	
	81, 79	5.56e−4	2.03	6.03e−3	1.22
	161, 159	1.39e−4	2.00	2.32e−3	1.38
	321, 319	3.66e−5	1.92	1.03e−3	1.17
$\phi = \phi_2$	40, 40	1.79e−3		1.39e−2	
	80, 80	4.83e−4	1.88	5.81e−3	1.26
	160, 160	1.26e−4	1.94	2.30e−3	1.34
	320, 320	3.27e−5	1.94	1.03e−3	1.16
	41, 39	1.89e−3		1.43e−2	
	81, 79	5.04e−4	1.91	6.19e−3	1.20
	161, 159	1.32e−4	1.93	2.33e−3	1.41
	321, 319	3.38e−5	1.97	1.07e−3	1.12

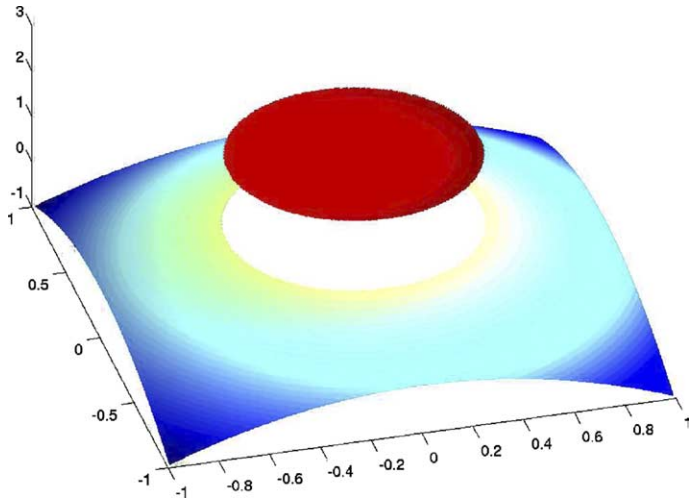

Fig. 3. Difficulty: The ratio β^+/β^- is very small.

$$\phi = x^2 + y^2 - 0.25,$$
(a) $\beta^+ = 10^3, \quad \beta^- = 1,$
(b) $\beta^+ = 1, \quad \beta^- = 10^3,$
(c) $\beta^+ = 10^6, \quad \beta^- = 1,$
(d) $\beta^+ = 1, \quad \beta^- = 10^6,$

$$u^+ = \frac{r^\alpha}{\beta^+} + \left(\frac{1}{\beta^-} - \frac{1}{\beta^+}\right) r_0^\alpha, \quad u^- = \frac{r^\alpha}{\beta^-},$$

Table 2
2nd order in u and 1st order in ∇u

# of pts in x, y	Err in U	Order	Err in ∇U	Order
40, 40	5.54e−1		3.92e−0	
80, 80	1.45e−1	1.93	1.34e−0	1.55
160, 160	3.19e−2	2.18	6.43e−1	1.06
320, 320	8.94e−3	1.84	2.84e−1	1.18
41, 39	4.91e−1		3.92e−0	
81, 79	1.37e−1	1.84	1.57e−0	1.32
161, 159	3.84e−2	1.83	5.59e−1	1.49
321, 319	9.04e−3	2.09	2.98e−1	0.91

where $\alpha = 3$, $r = \sqrt{x^2 + y^2}$, and $r_0 = 0.5$, see the example in [7]. Fig. 4 shows the numerical solution of the method in solving case (c) using 513 number of points in both x and y directions. The difficulty of the example is that $\beta^+/\beta^- \approx 10^{+3}$ (case (a)), 10^{-3} (case (b)), 10^{+6} (case (c)) or 10^{-6} (case (d)), which are either very large or small. Table 3 shows that the method achieves 2nd order accuracy in solutions and first order accuracy in its gradient in all four cases. The errors in all four cases are of the same magnitude, which means the method is not very sensitive to $\beta^{\pm}$.

Example 4. The level-set function ϕ, the coefficients $\beta^{\pm}$ and the solution $u^{\pm}$ are given as follows:

$$\phi = x^2 + y^2 - 0.25,$$
$$\beta^+ = b, \quad \beta^- = r^2 + 1,$$
$$u^+ = 1/4 + \frac{\frac{r^4}{2} - \frac{1}{32}}{b} + \frac{r^2 - \frac{1}{4}}{b} + \frac{C}{b}\log(2r) \quad u^- = r^2,$$

where $r = \sqrt{x^2 + y^2}$, see the example in [5]. Two cases are studied here: (a) $b = 10$ and $C = 0.1$; (b) $b = -3$ and $C = 0.1$. Note that in the case (b) $\beta^+ = -3 < 0$, the problem is not formally an elliptic problem (but could be converted to be an elliptic problem). Fig. 5 shows the numerical solutions of the method in solving case (a) and case (b) using 321 number of points in both x and y directions. The difficulty of the example is

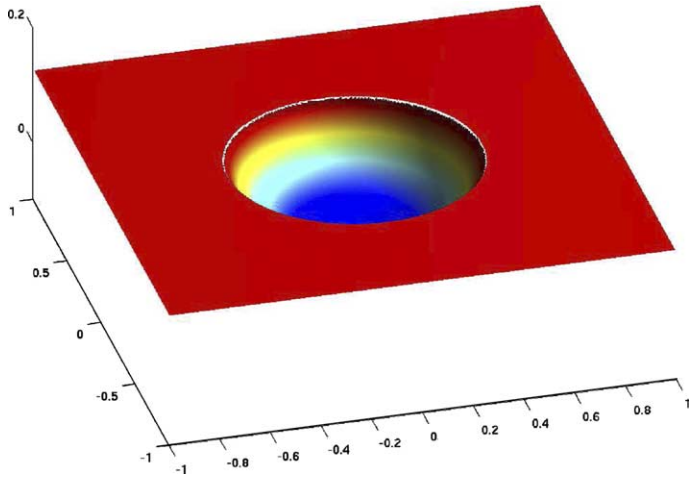

Fig. 4. Difficulty: The ratio β^+/β^- is very small.

Table 3
2nd order in u and 1st order in ∇u

Cases	# of pts in x, y	Err in U	Order	Err in ∇U	Order
case (a) $\beta^- = 1$ $\beta^+ = 10^3$	65, 65	4.96e−4		1.93e−3	
	129, 129	1.46e−4	1.76	5.98e−4	1.69
	257, 257	3.92e−5	1.90	2.35e−4	1.35
	513, 513	1.00e−5	1.97	1.06e−4	1.15
case (b) $\beta^- = 10^3$ $\beta^+ = 1$	65, 65	6.19e−4		3.10e−3	
	129, 129	1.42e−4	2.14	9.59e−4	1.69
	257, 257	3.82e−5	1.89	3.72e−4	1.37
	513, 513	9.32e−6	2.04	1.43e−4	1.38
case (c) $\beta^- = 1$ $\beta^+ = 10^6$	65, 65	8.96e−4		2.29e−3	
	129, 129	2.13e−4	2.07	7.92e−4	1.53
	257, 257	6.20e−5	1.78	4.34e−4	0.87
	513, 513	1.59e−5	1.96	2.67e−4	0.70
case (d) $\beta^- = 10^6$ $\beta^+ = 1$	65, 65	6.71e−4		3.88e−3	
	129, 129	1.93e−4	1.80	1.33e−3	1.54
	257, 257	5.02e−5	1.94	5.61e−4	1.25
	513, 513	1.26e−5	1.99	2.67e−4	1.07

that the problem is not formally elliptic in case (b), since $\beta^+ = -3 < 0$. Table 4 shows that the method achieves 2nd order accuracy in solutions and first order accuracy in its gradient in case (a).

Example 5. The level-set function ϕ, the coefficients $\beta^{\pm}$ and the solution $u^{\pm}$ are given as follows:

$$\phi = (x - 0.02\sqrt{5})^2 + (y - 0.02\sqrt{5})^2 - (0.5 + 0.2\sin(5\theta))^2,$$

$$\text{with} \begin{cases} x(\theta) = 0.02\sqrt{5} + (0.5 + 0.2\sin(5\theta))\cos(\theta), \\ y(\theta) = 0.02\sqrt{5} + (0.5 + 0.2\sin(5\theta))\sin(\theta), \end{cases} \quad \theta \in [0, 2\pi),$$

$$\beta^+ = (xy + 2)/5, \quad \beta^- = (x^2 - y^2 + 3)/7,$$

$$u^+ = 5 - 5x^2 - 5y^2, \quad u^- = 7x^2 + 7y^2 + 6.$$

The difficulty of the example is that the interface has complicated geometry. Fig. 6 shows the numerical solution of the method using 321 number of points both in x and y directions. Table 5 shows that the method achieves 2nd order accuracy in solutions and 1st order accuracy in its gradients on two different sets of grids. The method is not sensitive to the grids.

Example 6. The level-set function ϕ, the coefficients $\beta^{\pm}$ and the solution $u^{\pm}$ are given as follows:

$$\phi = x^2 - y - 1,$$

$$\beta^+ = xy + 2, \quad \beta^- = x^2 - y^2 + 3,$$

$$u^+ = 4 - x^2 - y^2, \quad u^- = x^2 + y^2.$$

Also note that the interface is tangential to the boundary $\partial\Omega$ at (0,1) point, and it intersects with the boundary $\partial\Omega$ at (−1,0) and (1,0) at certain nonzero angles. The difficulty of the example is that the interface is tangential to the boundary and intersects with the boundary at certain nonzero angles. Fig. 7 shows the

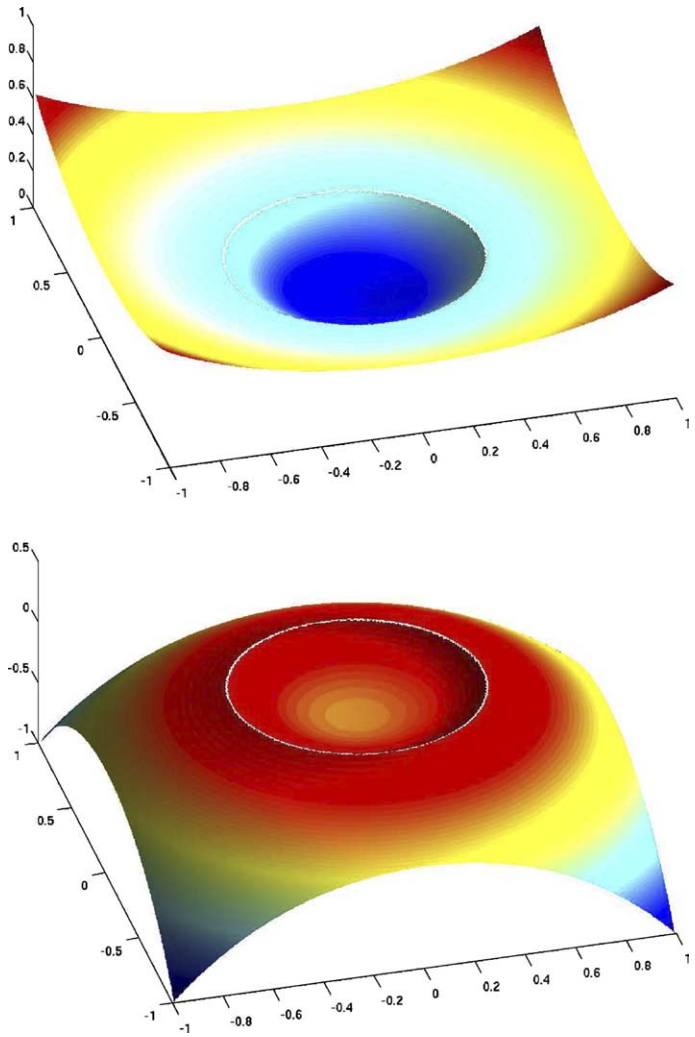

Fig. 5. Upper part is case (a); Lower part is case (b), which has $\beta^+ = -3 < 0$.

Table 4
2nd order in u and 1st order in ∇u in case (a)

# of pts in x, y	Err in U	Order	Err in ∇U	Order
21, 21	1.27e−3		2.24e−3	
41, 41	3.13e−4	2.02	6.36e−4	1.82
81, 81	7.17e−5	2.13	2.03e−4	1.65
161, 161	1.82e−5	1.98	6.94e−5	1.55
321, 321	4.42e−6	2.04	2.86e−5	1.28

numerical solution of the method using 321 number of points both in x and y directions. Table 6 shows that the method still achieves 2nd order accuracy in solutions and about 1st order accuracy in its gradients on two different sets of grids. The method is not sensitive to the grids.

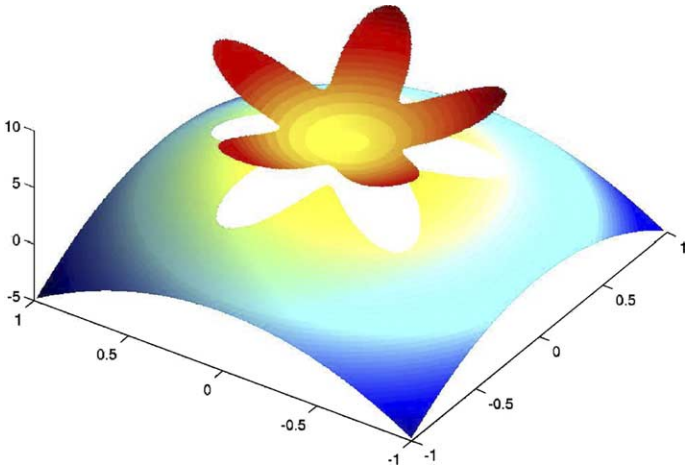

Fig. 6. Difficulty: more complicated geometry of the interface.

Table 5
2nd order in u and 1st order in ∇u

# of pts in x, y	Err in U	Order	Err in ∇U	Order
40, 40	3.18e−2		1.48e−1	
80, 80	9.02e−3	1.82	1.32e−1	0.17
160, 160	2.08e−3	2.12	4.79e−2	1.46
320, 320	5.55e−4	1.91	2.05e−2	1.22
41, 39	2.75e−2		2.73e−1	
81, 79	9.28e−3	1.57	1.61e−1	0.76
161, 159	2.54e−3	1.87	4.19e−2	1.94
321, 319	5.67e−4	2.16	2.72e−2	0.62

4.2. Lipschitz continuous interface and smooth solutions

In all experiments of this subsection, all interfaces are only Lipschitz continuous or worse, solutions are $C^{\infty}(\overline{\Omega^{\pm}})$ and the domains are $(-1,1)\times(-1,1)$.

Recall that the interface in the interface cell K is approximated by a straight line segment Γ_K^h, which is a good approximation if there is no kink located inside of any cell, and is not a good approximation if the interface has a kink in side of one cell. It is accurate enough to achieve 2nd order accuracy in L^{∞} for the extension U^h and hence the method, provided that there is only one smooth piece of interface in each cell K, i.e., all kinks are located on the edges of cells. Our numerical experiments below confirm that. On the other hand, if there is one interface cell consisting more than one smooth piece of interface, i.e., the kink is inside of the cell, the order of accuracy of the method will degrade, as shown below. However the numerical experiments suggest that the numerical solutions converge. This is the 1st convergent method in the literature on the problem (2.1a)–(2.1c) with Lipschitz continuous interfaces.

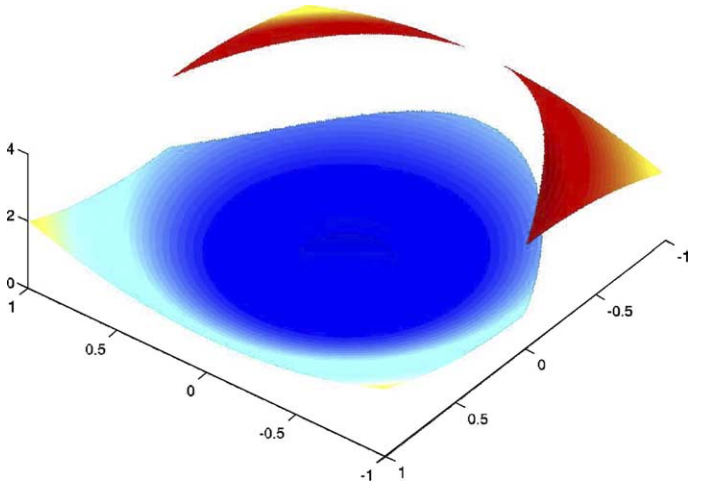

Fig. 7. Difficulty: Γ is smooth but is tangential to $\partial\Omega$ and intersects with $\partial\Omega$ with non-zero angles.

Table 6
2nd order in u and 1st order in ∇u

# of pts in x, y	Err in U	Order	Err in ∇U	Order
40, 40	4.88e−4		2.70e−3	
80, 80	1.25e−4	1.96	1.11e−3	1.28
160, 160	3.40e−5	1.88	7.02e−4	0.66
320, 320	8.99e−6	1.92	4.59e−4	0.61
41, 39	5.05e−4		2.95e−3	
81, 79	1.35e−4	1.90	1.20e−3	1.30
161, 159	3.51e−5	1.94	5.88e−4	1.03
321, 319	9.05e−6	1.96	2.89e−4	1.02

Example 7. The level-set function ϕ, the coefficients $\beta^{\pm}$ and the solution $u^{\pm}$ are given as follows:

$$\phi = (3(x^2+y^2)-x)^2 - x^2 - y^2 \quad \text{(cardioid)},$$
$$\beta^+ = x^2 - y^2 + 3, \quad \beta^- = xy + 3,$$
$$u^+ = 1 - x^2 - y^2, \quad u^- = x^2 + y^2 + 2.$$

Note that the interface is not even Lipschitz continuous and the singular point of the interface is the cusp point (0,0). The difficulty is that the interface is not even Lipschitz continuous. Fig. 8 shows the numerical solution of the method using 321 number of points both in x and y directions. The numerical accuracy tests seems to suggest that 1.8th order accurate convergence in solutions and about 1st order in ∇u on two different sets of grids, see Table 7.

Example 8. The level-set function ϕ, the coefficients $\beta^{\pm}$ and the solution $u^{\pm}$ are given as follows:

$$\phi = (\sin(5\pi x) - y)(-\sin(5\pi y) - x),$$
$$\beta^+ = xy + 2, \quad \beta^- = x^2 - y^2 + 3,$$
$$u^+ = 4 - x^2 - y^2, \quad u^- = x^2 + y^2.$$

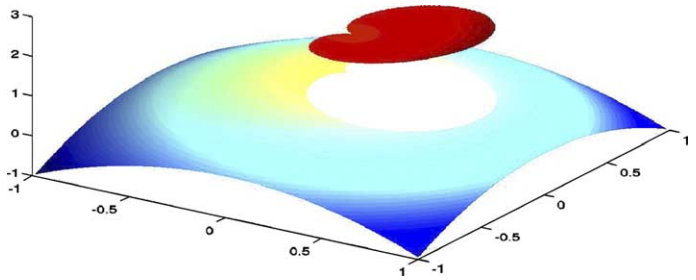

Fig. 8. Γ is a cardioid and is not Lipschitz continuous at the cusp point, (0,0), of the cardioid.

Table 7
About 1.8th order in u and about 1st order in ∇u

# of pts in x, y	Err in U	Order	Err in ∇U	Order
40, 40	4.08e−3		2.02e−2	
80, 80	7.90e−4	2.36	8.00e−3	1.34
160, 160	2.14e−4	1.88	4.05e−3	0.98
320, 320	1.48e−4	0.53	3.46e−3	0.23
640, 640	7.77e−5	2.70	2.45e−3	0.50
41, 39	3.60e−3		1.94e−2	
81, 79	9.85e−4	1.87	6.52e−3	1.57
161, 159	2.96e−4	1.73	3.56e−3	0.87
321, 319	6.77e−5	2.13	1.54e−3	1.21
641, 639	2.43e−5	1.48	6.31e−4	1.29

The difficulty of the example is that there are many kinks on the interface and some of their coordinates are irrational. There is no way to construct a uniform grid to make sure that every triangle cell has only one smooth piece interface. That is the reason why the method is only 0.8th order accurate, see Table 8. Also see Fig. 9 for the numerical solution of the method using 321 number of points both in x and y directions.

Example 9. The level-set function ϕ, the coefficients $\beta^{\pm}$ and the solution $u^{\pm}$ are given as follows:

$$\phi = \max(\min(\phi_1, \phi_2, \phi_3), \phi_4, \phi_5, \phi_6, \min(\phi_7, \phi_8)),$$

$$\begin{cases} \phi_1 = \sqrt{x^2 + y^2 - 0.75^2 - 0.15^2}, \\ \phi_2 = (x - 0.75)^2 + y^2 - 0.15^2, \\ \phi_3 = (x + 0.75)^2 + y^2 - 0.15^2, \\ \phi_4 = -\frac{0.1}{0.12}(x - 0.2)^2 - \frac{0.12}{0.1}(y - 0.22)^2 + 0.12 \cdot 0.1, \\ \phi_5 = -\frac{0.1}{0.12}(x + 0.2)^2 - \frac{0.12}{0.1}(y - 0.22)^2 + 0.12 \cdot 0.1, \\ \phi_6 = -x^2 - (y + 0.08)^2 + 0.12^2, \\ \phi_7 = -x^2 - (y + 0.625)^2 + 0.425^2, \\ \phi_8 = -x^2 - (y + 0.25)^2 + 0.2^2, \end{cases}$$

$$\beta^+ = (xy + 2)/5, \quad \beta^- = (x^2 - y^2 + 3)/7,$$

$$u^+ = 5 - 5x^2 - 5y^2, \quad u^- = 7x^2 + 7y^2 + 1.$$

Table 8
0.8th order in u

# of pts in x, y	Err in U	Order
40, 40	2.38e−1	
80, 80	7.88e−2	1.59
160, 160	5.43e−2	0.54
320, 320	2.57e−2	1.08
41, 39	1.24e−1	
81, 79	6.75e−2	0.88
161, 159	4.56e−2	0.57
321, 319	2.25e−2	1.02

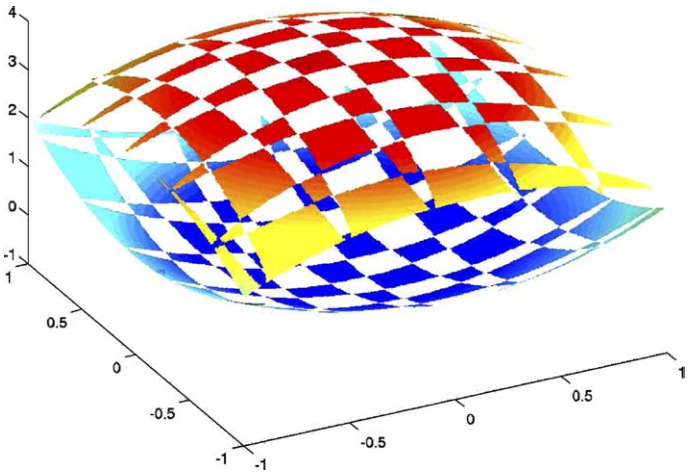

Fig. 9. Γ has many kinks and intersects with the outer boundary $\partial\Omega$.

Note that the interfaces have kinks around ears and mouth, and the mouth and the nose are tangential at point (0,−0.2), which is not Lipschitz continuous (see Fig. 10). Fig. 10 shows the numerical solution using 321 number of points both in x and y directions. Table 9 shows the results of numerical accuracy tests. Because all kinks and the touch point (0,−0.2) are on grid points, and hence every interface cell has only one smooth piece interface. Our method achieve 2nd order accuracy in solutions and more than 1st order accuracy in its gradients. The cases that the kinks of interfaces are not all on the cell boundaries, are studied in the Section 4.4.

4.3. Piecewise C^2, C^1 Solutions with C^2, C^1 Interfaces

Two interfaces are used:

$$\phi = \begin{cases} y - (2x + x^2), & x + y > 0, \\ y - (x + x^2 + \sin(5x)/5), & x + y \leqslant 0 \end{cases} \tag{4.1a}$$

and

$$\phi = \begin{cases} y - (2x), & x + y > 0, \\ y - (2x + x^2), & x + y \leqslant 0. \end{cases} \tag{4.1b}$$

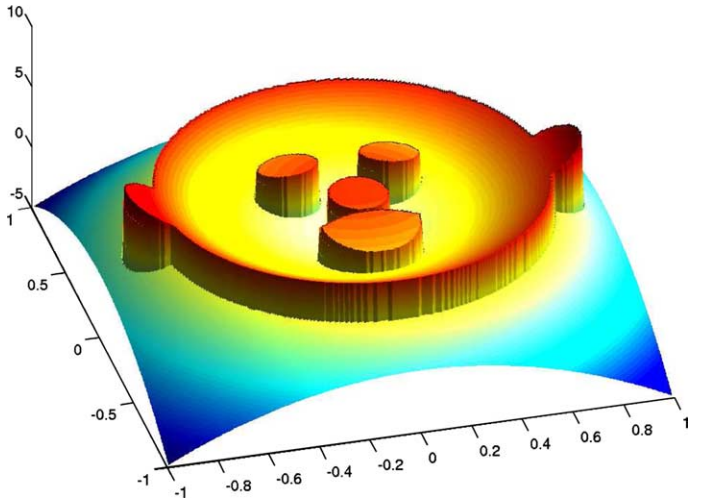

Fig. 10. Γ has many kinks at the corners of ears, the corners of mouth, and the touching point of the nose and the mouth.

Table 9
2nd order in u and more than 1st order in ∇u

# of pts in x, y	Err in U	Order	Err in ∇U	Order
40, 40	6.06e−2		3.09e−1	
80, 80	1.64e−2	1.89	1.16e−1	1.41
160, 160	4.34e−3	1.92	4.71e−2	1.30
320, 320	1.15e−3	1.92	1.81e−2	1.40

The 1st interface (4.1a) is C^2 but not C^3 and its non-C^3 point is (0,0). The 2nd interface (4.1b) is C^1 but not C^2 and its non-C^2 point is (0,0).

Two solutions are used:

$$u^+ = 2, \quad u^- = \begin{cases} \sin(x+y), & x+y \leqslant 0, \\ x+y, & x+y > 0, \end{cases} \tag{4.2a}$$

$$u^+ = 2, \quad u^- = \begin{cases} \sin(x+y)+\cos(x+y), & x+y \leqslant 0, \\ x+y+1, & x+y > 0. \end{cases} \tag{4.2b}$$

For ease of referring, the solution in (4.2a) is called piecewise C^2 in the following sense: $u \in C^2(\overline{\Omega^{\pm}}), \notin C^3(\overline{\Omega^{\pm}})$ with bounded 3rd derivatives. Its non-C^3 points in Ω^- are $\{(x,-x)|x>0\}$. For the same reason, the solution in (4.2b) is called piecewise C^1 in the following sense: $u \in C^1(\overline{\Omega^{\pm}}), \notin C^2(\overline{\Omega^{\pm}})$ with bounded 2nd derivatives. Its non-C^2 points in Ω^- are $\{(x,-x)|x>0\}$.

One domain is used: $(-1,\pi-2)\times(-1,\pi-2)$. A sequence of uniform Cartesian grids on this domain is used:

$$\Omega^k = \left\{ (x_i^k, y_j^k) \middle| \begin{matrix} x_i^k = -1 + i\Delta x^k, \ i = 0,\ldots,2^k 10+1, \\ y_j^k = -1 + j\Delta y^k, \ j = 0,\ldots,2^k 10-1, \end{matrix} \right\} \tag{4.3}$$

where $\Delta x^k = \frac{\pi-1}{2^k 10+1}$ and $\Delta y^k = \frac{\pi-1}{2^k 10-1}$. Note that the non-smooth point (0,0) of the interfaces will not locate on the edges of triangles of the triangulations resulting from the sequence of uniform Cartesian grids.

Example 10. The level-set function ϕ, the coefficients $\beta^{\pm}$ and the solution $u^{\pm}$ are given as follows:

$$\phi = \begin{cases} y - (2x + x^2), & x + y > 0, \\ y - (x + x^2 + \sin(5x)/5), & x + y \leqslant 0, \end{cases}$$
$$\beta^+ = (xy + 2)/5, \quad \beta^- = (x^2 - y^2 + 3)/7,$$
$$u^+ = 2, \quad u^- = \begin{cases} \sin(x + y), & x + y \leqslant 0, \\ x + y, & x + y > 0. \end{cases}$$

Note that the interface is C^2 but not C^3 and the solution u is piecewise C^2. Fig. 11 shows the numerical solution using Ω^5 of (4.3). Table 10 shows that the method achieves 2nd order accuracy in solutions and 1st order accuracy in its gradient.

Example 11. The level-set function ϕ, the coefficients $\beta^{\pm}$ and the solution $u^{\pm}$ are given as follows:

$$\phi = \begin{cases} y - (2x + x^2), & x + y > 0, \\ y - (x + x^2 + \sin(5x)/5), & x + y \leqslant 0, \end{cases}$$
$$\beta^+ = (xy + 2)/5, \quad \beta^- = (x^2 - y^2 + 3)/7,$$
$$u^+ = 2, \quad u^- = \begin{cases} \sin(x + y) + \cos(x + y), & x + y \leqslant 0, \\ x + y + 1, & x + y > 0. \end{cases}$$

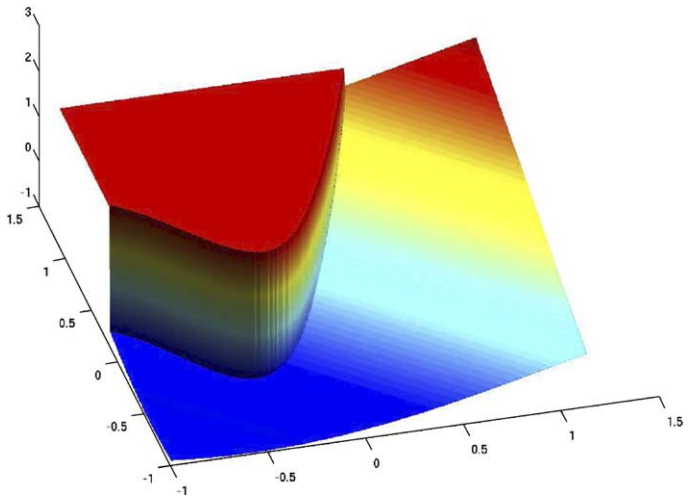

Fig. 11. Interface is C^2 but not C^3 and u^- is piecewise C^2. The non-C^3 point (0,0) of the interface is on the non-C^3 points, $\{(x,-x)|x > 0\}$, of the solution.

Table 10
2nd order in u and 1st order in ∇u

# of pts in x, y	Err in U	Order	Err in ∇U	Order
41,39	7.05e−4		5.03e−3	
81,79	2.51e−4	1.49	2.30e−3	1.13
161, 159	6.16e−5	2.03	9.15e−4	1.33
321, 319	1.76e−5	1.81	4.46e−4	1.04
641, 639	3.98e−6	1.93	1.91e−4	1.10

Note that the interface Γ is C^2 but not C^3 and the solution u is C^1 but not C^2 on $\overline{\Omega^-}$. Fig. 12 shows the numerical solution using Ω^5 of (4.3). Table 11 shows that the method achieves 1st order accuracy in solutions and about 0.8th order accuracy in its gradient.

Example 12. The level-set function ϕ, the coefficients $\beta^{\pm}$ and the solution $u^{\pm}$ are given as follows:

$$\phi = \begin{cases} y-(2x), & x+y>0, \\ y-(2x+x^2), & x+y\leqslant 0, \end{cases}$$
$$\beta^+ = (xy+2)/5, \quad \beta^- = (x^2-y^2+3)/7,$$
$$u^+ = 2, \quad u^- = \begin{cases} \sin(x+y), & x+y\leqslant 0, \\ x+y, & x+y>0. \end{cases}$$

Note that the interface is C^1 but not C^2 and the solution u is C^2 but not C^3 on $\overline{\Omega^-}$. Fig. 13 shows the numerical solution using Ω^5 grid of (4.3). Table 12 shows that the method achieves 2nd order accuracy in solutions and 1st order accuracy in its gradients.

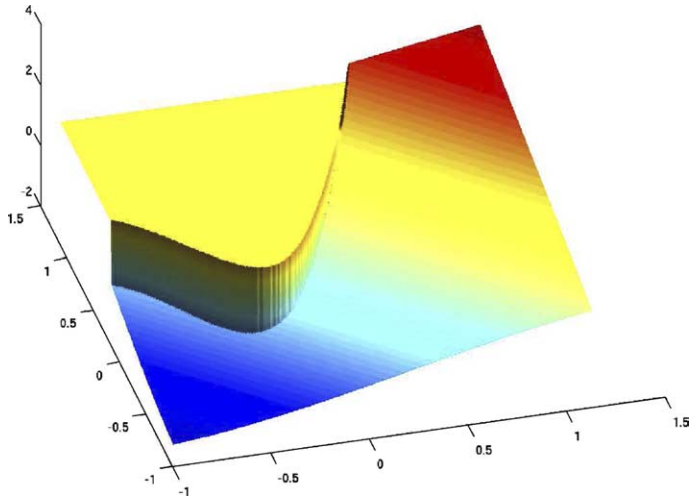

Fig. 12. Interface is C^2 but not C^3 and u^- is piecewise C^1. The non-C^3 point (0,0) of the interface is on the non-C^2 points, $\{(x,-x)|x>0\}$, of the solution.

Table 11
1st order in u and about 0.8th order in ∇u

# of pts in x, y	Err in U	Order	Err in ∇U	Order
41,39	1.54e−3		1.78e−2	
81,79	7.75e−4	0.99	9.30e−3	0.94
161,159	5.06e−4	0.62	5.46e−3	0.77
321,319	2.02e−4	1.32	3.62e−3	0.59
641,639	7.72e−5	1.00	1.99e−3	0.76

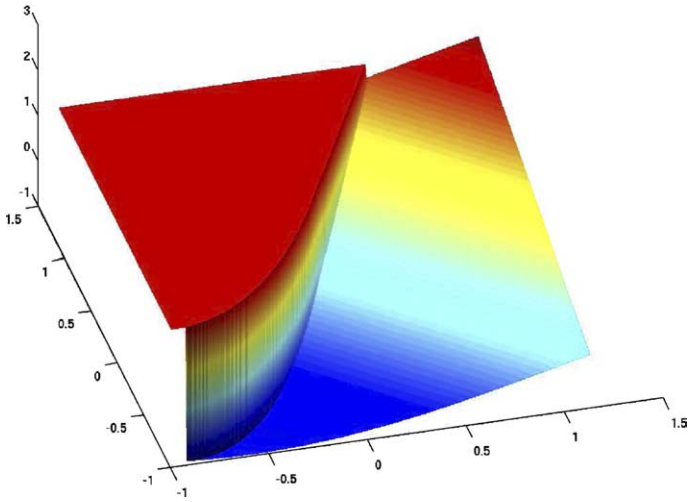

Fig. 13. Interface is C^1 but not C^2 and u^- is piecewise C^2. The non-C^2 point (0,0) of the interface is on the non-C^3 points, $\{(x,-x)|x > 0\}$, of the solution.

Table 12
About 2nd order in u and 1st order in ∇u

# of pts in x, y	Err in U	Order	Err in ∇U	Order
41, 39	2.74e−4		1.42e−3	
81, 79	7.89e−5	1.80	5.49e−4	1.37
161, 159	2.29e−5	1.78	3.70e−4	0.57
321, 319	6.17e−6	1.89	1.40e−4	1.40
641, 639	1.71e−6	1.85	7.60e−5	0.88

Example 13. The level-set function ϕ, the coefficients $\beta^{\pm}$ and the solution $u^{\pm}$ are given as follows:

$$\phi = \begin{cases} y-(2x), & x+y>0, \\ y-(2x+x^2), & x+y\leqslant 0, \end{cases}$$
$$\beta^+ = (xy+2)/5, \quad \beta^- = (x^2-y^2+3)/7,$$
$$u^+ = 2, \quad u^- = \begin{cases} \sin(x+y)+\cos(x+y), & x+y\leqslant 0, \\ x+y+1, & x+y>0. \end{cases}$$

Note that the interface Γ is C^1 but not C^2 and the solution u is C^1 but not C^2 on $\overline{\Omega^-}$. Fig. 14 shows the numerical solution using Ω^5 grid of (4.3). Table 13 shows that the method achieves 1st order accuracy in solutions and about 0.8th order accuracy in its gradients.

4.4. Piecewise H^2 solutions and/or Lipschitz continuous interfaces

In the previous subsection, the interfaces used are either C^2 (but not C^3) or C^1 (but not C^2) and the solutions used is either piecewise C^2 or piecewise C^1.

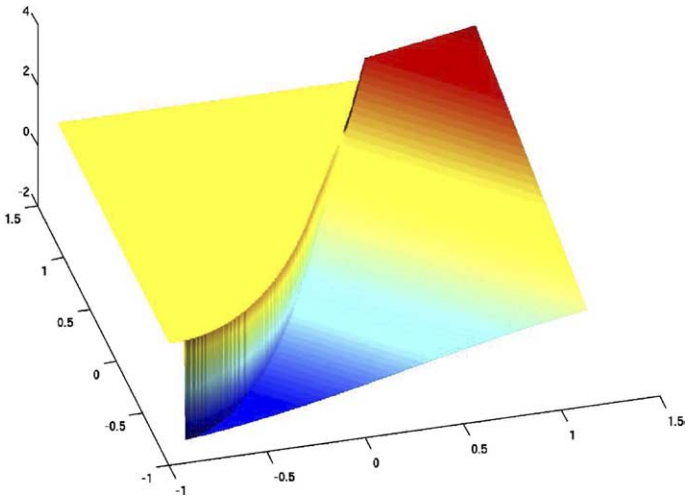

Fig. 14. Interface is C^1 but not C^2 and u^- is piecewise C^1. The non-C^2 point (0,0) of the interface is on the non-C^2 points, $\{(x,-x)|x>0\}$, of the solution.

Table 13
1st order in u and 0.8th order in ∇u

# of pts in x, y	Err in U	Order	Err in ∇U	Order
41, 39	1.35e−3		1.79e−2	
81, 79	7.80e−4	0.79	9.35e−3	0.94
161, 159	5.01e−4	0.64	5.45e−3	0.78
321, 319	2.03e−4	1.30	3.62e−3	0.59
641, 639	9.64e−5	1.07	2.02e−3	0.84

In this subsection, a Lipschitz continuous interface is used:

$$\phi = \begin{cases} y - 2x & x + y > 0, \\ y + \frac{1}{2}x & x + y \leqslant 0. \end{cases} \tag{4.4}$$

Clearly its singular point (kink) is the origin (0,0).

In the existence and uniqueness Theorem 2.1, the right hand side $f = \nabla \cdot (\beta \nabla u)$ is only required to be $L^2(\Omega)$ and could blow up at some point in Ω. In this subsection, a solution

$$u = \begin{cases} u^+ = 8, & \Omega^+, \\ u^- = (x^2 + y^2)^{\frac{5}{6}} + \sin(x + y), & \Omega^- \end{cases} \tag{4.5}$$

is used. For ease of referring, the solution in (4.5) is called piecewise H^2 in the following sense: $u^{\pm} \in H^2(\Omega^{\pm}), \in C^1(\overline{\Omega^{\pm}})$ with unbounded 2nd derivatives. Its singular point, where its 2nd derivatives blow up, is the origin (0,0). Since $\beta\pm \in C^{\infty}(\overline{\Omega^{\pm}})$, the resulting $f = \nabla \cdot (\beta \nabla u) \in L^2(\Omega)$ but blow up at the origin. An extra caution is needed: never evaluate f at its exact blow-up point.

All numerical experiments in this subsection possess a singular point either from the interface (4.4) and/or from the solution (4.5). At the singular cell, in which the interface has a singular point (kink) inside of the cell, integrations $\int_{K^{\pm}}$ and $\int_{\Gamma_K^h}$ in the Method 3.2 are not good approximations of their associated ones in the weak formulation (2.7), since Γ has a kink inside K and Γ_K^h is a straight line segment inside K. At the singular cell, in which solutions $u^{\pm} \notin C^2(\overline{\Omega^-})$ have a singular point and so is the f, the numerical quadrature used in evaluating $\int_K f T^h(\psi_{m,n}^h)$ in the Method 3.2 loses the 2nd order accuracy, so does the extension $U^h(u^h)$

in the Method 3.2. The order of accuracy of those approximations depends on the relative locations of the singular points in the singular cells. Hence the method under arbitrary sequences of grids will not show the order of accuracy in a consistent way.

Special but rather general sequences of uniform Cartesian grids are used, which require the relative locations of the singular points are the same or almost same in the singular cells of all grids within the same sequences. For ease of discussion, one dimensional case is considered first. Let $\Omega = (x_{\min}, x_{\max})$ be the domain with finite number of singular points: $x_{s_1}, \ldots, x_{s_L} \in \Omega$. Assume the singular points are at relatively rational locations, i.e., $\frac{x_{s_l} - x_{\min}}{x_{\max} - x_{\min}}$ are rational: $\frac{x_{s_l} - x_{\min}}{x_{\max} - x_{\min}} = \frac{p_l}{q_l}$ for $l = 1, \ldots, L$, where p and q are positive integers, $p < q$, p and q have no common factor other than 1, relevantly. A sequence $\{\Omega^m\}$ of uniform Cartesian grids can be constructed, in which each grid Ω^m is

$$\Omega^m = \{x_i^m = x_{\min} + i\Delta x^m,\ i = 0, 1, \ldots, I_m + 1\},$$

where $\Delta x^m = \frac{x_{\max} - x_{\min}}{I_m + 1}$, $I_m = r^m kQ$, $r > 1$, $k > 0$, $Q > 0$ are integers, and Q is the smallest multiple of all q_l. It is easy to check that $\frac{x_{s_l} - x^m_{\frac{p_l}{q_l} I_m}}{\Delta x^m} = \frac{x_{s_l} - x_{\min}}{x_{\max} - x_{\min}}$ holds for every Ω^m in the sequence $\{\Omega^m\}$. Note that $\frac{x_{s_l} - x_{\min}}{x_{\max} - x_{\min}}$ are independent from m. Therefore the relative location of each singular points, x_{s_l}, in the singular cell $[x_{\frac{p_l}{q_l} I_m}, x_{\frac{p_l}{q_l} I_m + 1}]$ of Ω^m is the same for all m.

For two dimensional case, let $\Omega = (x_{\min}, x_{\max}) \times (y_{\min}, y_{\max})$ be the domain with finite number of singular points: $(x_{s_1}, y_{s_1}), \ldots, (x_{s_L}, y_{s_L}) \in \Omega$. Assume the singular points are at relatively rational locations, i.e.,

$$\frac{x_{s_l} - x_{\min}}{x_{\max} - x_{\min}} = \frac{p_{x,l}}{q_{x,l}}, \quad \frac{y_{s_l} - y_{\min}}{y_{\max} - y_{\min}} = \frac{p_{y,l}}{q_{y,l}} \tag{4.6}$$

for $l = 1, \ldots, L$, where p and q are positive integers, $p < q$ and p and q have no common factor other than 1, relevantly. Two sequences, $\{\Omega^{x,m}\}$ and $\{\Omega^{y,n}\}$, of one dimensional uniform Cartesian grids can be constructed in each direction:

$$\Omega^{x,m} = \{x_i^m = x_{\min} + i\Delta x^m,\ i = 0, 1, \ldots, I_m + 1\},$$
$$\Omega^{y,n} = \{y_j^n = y_{\min} + j\Delta y^n,\ j = 0, 1, \ldots, J_n + 1\},$$

where $\Delta x^m = \frac{x_{\max} - x_{\min}}{I_m + 1}$, $\Delta y^n = \frac{y_{\max} - y_{\min}}{J_n + 1}$, $I_m = r^m k_x Q_x$, $J_n = r^n k_y Q_y$, $r > 1$, $k_x > 0$, $k_y > 0$, Q_x and Q_y are integers, and Q_x is the smallest multiple of $q_{x,1}, \ldots, q_{x,L}$ and Q_y is the smallest multiple of $q_{y,1}, \ldots, q_{y,L}$. The sequence of uniform Cartesian grids in two dimension $\{\Omega^{m,n}\}$ can be constructed, in which

$$\Omega^{m,n} = \Omega^{x,m} \times \Omega^{y,n} = \{(x_i^m, y_j^n) \mid x_i^m \in \Omega^{x,m}, y_j^n \in \Omega^{y,n}\}. \tag{4.7}$$

Three sequences of uniform Cartesian grids are used in all five numerical experiments in this subsection. First two of them are in the form of (4.7) and the third one is not:

$$\Omega^{k,k} = \left\{ (x_i^k, y_j^k) \middle| \begin{array}{l} x_i^k = -1 + i\Delta x^k,\ i = 0, \ldots, 2^k 10 + 1 \\ y_j^k = -1 + j\Delta y^k,\ j = 0, \ldots, 2^k 5 + 1 \end{array} \right\},$$
$$\text{where } \Delta x^k = \frac{4}{2^k 20 + 1} \quad \text{and} \quad \Delta y^k = \frac{2}{2^k 10 + 1} \tag{4.8a}$$

for the domain $(-1,3) \times (-1,1)$

$$\Omega^{k,k} = \left\{ (x_i^k, y_j^k) \middle| \begin{array}{l} x_i^k = \frac{-2\pi}{5} + i\Delta x^k,\ i = 0, \ldots, 2^k 20 + 1 \\ y_j^k = \frac{-2\pi}{5} + j\Delta y^k,\ j = 0, \ldots, 2^k 20 + 1 \end{array} \right\},$$
$$\text{where } \Delta x^k = \frac{\pi}{2^k 20 + 1} \quad \text{and} \quad \Delta y^k = \frac{\pi}{2^k 20 + 1} \tag{4.8b}$$

for the domain $(\frac{-2\pi}{5},\frac{3\pi}{5})\times(\frac{-2\pi}{5},\frac{3\pi}{5})$, and

$$\Omega^{k,k}=\left\{(x_i^k,y_j^k)\left|\begin{array}{l}x_i^k=-2+i\Delta x^k,\ i=0,\ldots,2^k\\ y_j^k=-1+j\Delta y^k,\ j=0,\ldots,2^k\end{array}\right.\right\},\quad \text{where } \Delta x^k=\frac{\frac{3\pi}{4}+2}{2^k}\quad\text{and}\quad \Delta y^k=\frac{\frac{4\pi}{5}+1}{2^k}\tag{4.8c}$$

for the domain $(-1,\frac{4\pi}{5})\times(-1,\frac{3\pi}{4})$.

Clearly the relative location of the singular point, the origin (0,0), is rational for the first two sequences (4.8a) and (4.8b) but irrational for the third one (4.8c).

Remark 7.

(1) In all five experiments in this subsection, the method is shown to be convergent under the grids (4.8c), although varying orders of accuracy have been observed. The grids (4.8a) and (4.8b) are used to see the orders of accuracy in a consistent way.
(2) The relative locations of singular points may be irrational, i.e. at least one of $\frac{x_{s_l}-x_{\min}}{x_{\max}-x_{\min}}$ and $\frac{y_{s_l}-y_{\min}}{y_{\max}-y_{\min}}$ is not rational number. However any irrational number is a limit of a sequence of rational numbers, hence can be approximated by a rational number. Therefore the grids (4.8c) is used in all five experiments.
(3) If the smallest multiple of all q is too large, a smaller integer is recommended, as long as the relative locations of the singular points do not vary too much.
(4) The sequences of grids (4.7) can handle the cases that there are finite number of singular points.

Example 14. The level-set function ϕ, the coefficients $\beta^{\pm}$ and the solution $u^{\pm}$ are given as follows:

$$\phi=\begin{cases}y-(2x+x^2), & x+y>0,\\ y-(x+x^2+\sin(5x)/5), & x+y\leqslant 0,\end{cases}$$
$$\beta^+=1,\quad \beta^-=2+\sin(x+y),$$
$$u^+=8,\quad u^-=(x^2+y^2)^{\frac{5}{6}}+\sin(x+y).$$

Note that the interface Γ is C^2 but not C^3 and the solution u is piecewise H^2. Note that $u^-\in H^2(\Omega^-),\in C^1(\overline{\Omega^-})$ and $u^-\notin C^2(\overline{\Omega^-})$. u and hence f have the singular point at the origin, which coincides with the interface non-C^3 point. Fig. 15 shows the numerical solution of the method using $\Omega^{5,5}$ of (4.8a) on the domain $(-1,3)\times(-1,1)$. Table 14 shows that the method achieves about 1.6th order accuracy in solutions and about 0.65th order accuracy in its gradient. Since $u\in H^2(\Omega^{\pm}),\in C^1(\overline{\Omega^{\pm}})$ but $u\notin C^2(\overline{\Omega^{\pm}})$, the linear interpolations $U^h(u^h)$ do not guarantee 2nd order accuracy in approximating the true solutions u. Varying orders of accuracy are observed under the grids (4.8c) since the singular point is not at relatively same locations in singular cells of the grids in the sequence (4.8c).

Example 15. The level-set function ϕ, the coefficients $\beta^{\pm}$ and the solution $u^{\pm}$ are given as follows:

$$\phi=\begin{cases}y-2x, & x+y>0,\\ y-(2x+x^2), & x+y\leqslant 0,\end{cases}$$
$$\beta^+=1,\quad \beta^-=2+\sin(x+y),$$
$$u^+=8,\quad u^-=(x^2+y^2)^{\frac{5}{6}}+\sin(x+y).$$

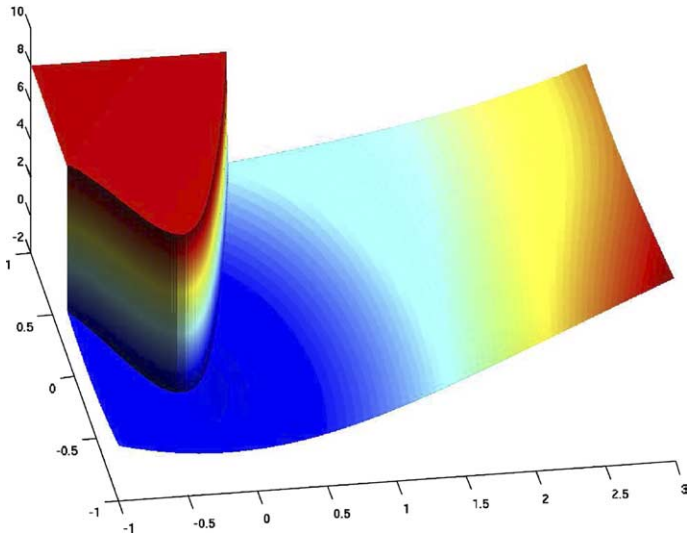

Fig. 15. Interface is C^2 but not C^3, its non-C^3 point is (0,0). u is piecewise H^2 and has a singular point at (0,0), which coincides with the interface non-C^3.

Table 14
About 1.6th order in u and about 0.65th order in ∇u

Domain	# of pts in x, y	Err in U	Order	Err in ∇U	Order
$(-1,3)\times(-1,1)$	81, 41	1.13e−3		1.22e−1	
	161, 81	3.69e−4	1.61	7.86e−2	0.63
	321, 161	1.22e−4	1.60	5.01e−2	0.65
	641, 321	4.02e−5	1.60	3.17e−2	0.66
$(\frac{-2\pi}{5},\frac{3\pi}{5})\times(\frac{-2\pi}{5},\frac{3\pi}{5})$	41, 41	2.09e−3		1.85e−1	
	81, 81	6.71e−4	1.64	1.20e−1	0.62
	161, 161	2.18e−4	1.62	7.61e−2	0.66
	321, 321	7.11e−5	1.62	4.81e−2	0.66
$(-2,\frac{3\pi}{4})\times(-1,\frac{4\pi}{5})$	128, 128	5.71e−4		1.27e−1	
	256, 256	1.65e−4	1.79	6.42e−2	0.98
	512, 512	4.33e−5	1.93	4.18e−2	0.62

Note that the interface Γ is C^1 but not C^2 and its non-C^2 point locates at (0,0). Also the solution u is piecewise $H^2(\Omega^{\pm})$ and has a singular point (0,0), which coincides with the interface non-C^2 point. Fig. 16 shows the numerical solution of the method using $\Omega^{5,5}$ of (4.8a) on the domain $(-1,3)\times(-1,1)$. Table 15 shows that the method achieves about 1.6th order accuracy in solutions and around 0.65th order accuracy in the gradient of the solutions. Since u is piecewise H^2 but not C^2 on $\overline{\Omega^-}$, the linear interpolations $U^h(u^h)$ do not guarantee 2nd order accuracy in approximating the true solutions u. Therefore the method degenerates from 2nd order accuracy. Varying orders of accuracy are observed under the grids (4.8c), since the singular point is not at relatively same locations in singular cells of the every grids in the sequence (4.8c).

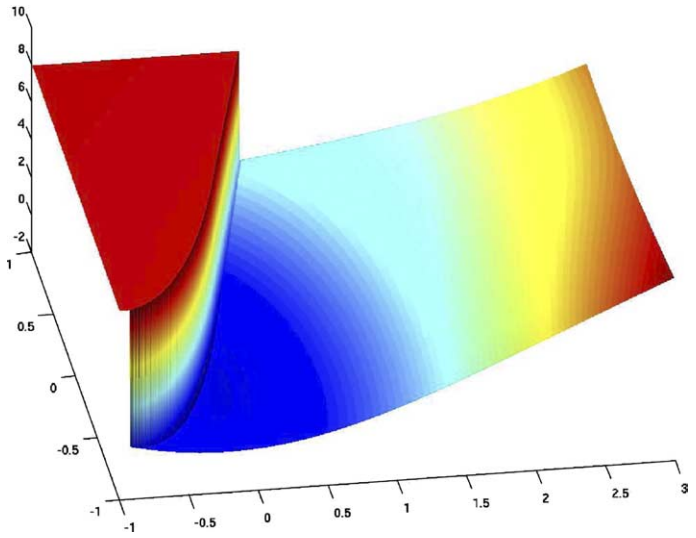

Fig. 16. Interface is C^1 but not C^2, its non-C^2 point is (0,0). u is piecewise H^2 and has a singular point at (0,0), which coincides with the interface non-C^2 point.

Table 15
About 1.6th order in u and about 0.65th order in ∇u

Domain	# of pts in x, y	Err in U	Order	Err in ∇U	Order
$(-1,3)\times(-1,1)$	81, 41	1.11e−3		1.23e−1	
	161, 81	3.58e−4	1.63	7.92e−2	0.64
	321, 161	1.16e−4	1.63	5.03e−2	0.65
	641, 321	3.81e−5	1.61	3.18e−2	0.66
$(\frac{-2\pi}{5},\frac{3\pi}{5})\times(\frac{-2\pi}{5},\frac{3\pi}{5})$	41, 41	2.10e−3		1.84e−1	
	81, 81	6.59e−4	1.67	1.19e−1	0.63
	161, 161	2.10e−4	1.65	7.57e−2	0.65
	321, 321	6.74e−5	1.64	4.79e−2	0.66
$(-2,\frac{3\pi}{4})\times(-1,\frac{4\pi}{5})$	128,128	4.00e−4		1.30e−1	
	256, 256	1.43e−4	1.48	6.45e−2	1.01
	512, 512	3.84e−5	1.90	4.21e−2	0.62

Example 16. The level-set function ϕ, the coefficients $\beta^{\pm}$ and the solution $u^{\pm}$ are given as follows:

$$\phi = \begin{cases} y - 2x, & x + y > 0, \\ y + \frac{1}{2}x, & x + y \leqslant 0, \end{cases}$$
$$\beta^{+} = (xy + 2)/5, \quad \beta^{-} = (x^2 - y^2 + 3)/7,$$
$$u^{+} = 8, \quad u^{-} = \begin{cases} \sin(x + y), & x + y \leqslant 0, \\ x + y, & x + y > 0. \end{cases}$$

Note that the interface Γ is Lipschitz continuous but not C^1 and and it has a kink at (0,0). The solution u is piecewise C^2 and the kink of the interface is on the non-C^3 points, $\{(x,-x)|x < 0\}$, of the solution. Fig. 17 shows the numerical solution using $\Omega^{5,5}$ of (4.8a) on the domain $(-1,3)\times(-1,1)$. Table 16 shows that the

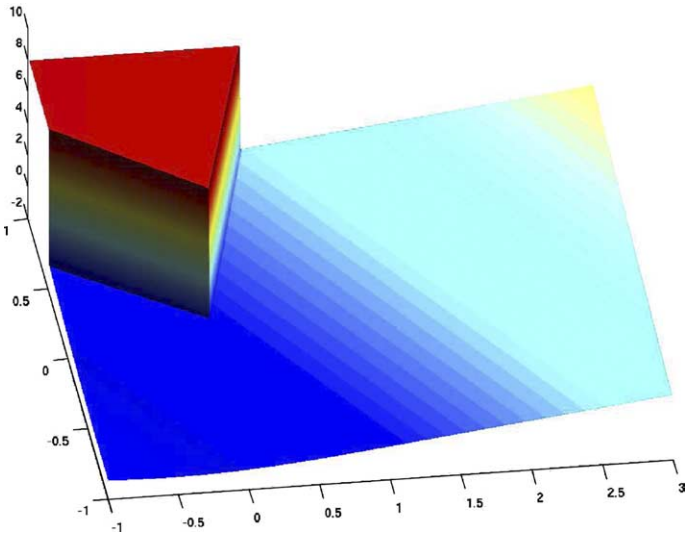

Fig. 17. Interface is Lipschitz continuous and it has a kink at (0,0). u is piecewise C^2. The kink (0,0) of the interface is on the non-C^3 points, $\{(x,-x)|x > 0\}$, of the solution.

Table 16
About 0.8th order in u

Domain	# of pts in x, y	Err in u	Order	Err in ∇u
$(-1,3)\times(-1,1)$	81,41	1.74e−2		1.14e−1
	161, 81	1.01e−2	0.78	1.14e−1
	321, 161	5.72e−3	0.82	1.15e−1
	641, 321	3.19e−3	0.84	1.15e−1
$(-\frac{2\pi}{5},\frac{3\pi}{5})\times(-\frac{2\pi}{5},\frac{3\pi}{5})$	41,41	2.17e−2		9.15e−2
	81,81	1.27e−2	0.77	9.41e−2
	161, 161	7.21e−3	0.82	9.47e−2
	321, 321	4.04e−3	0.84	9.49e−2
$(-2,\frac{3\pi}{4})\times(-1,\frac{4\pi}{5})$	128, 128	7.26e−2		1.15e−0
	256, 256	6.44e−2	0.17	2.29e−0
	512, 512	8.82e−3	2.87	5.60e−1

method achieves about 0.8th order accuracy in solutions on the whole domain. Varying orders of accuracy are observed under the grids (4.8c), since the singular point is not at relatively same locations in singular cells of the grids in the sequence (4.8c).

Example 17. The level-set function ϕ, the coefficients $\beta^{\pm}$ and the solution $u^{\pm}$ are given as follows:

$$\phi = \begin{cases} y - 2x, & x + y > 0, \\ y + \frac{1}{2}x, & x + y \leqslant 0, \end{cases}$$

$$\beta^{+} = (xy + 2)/5, \quad \beta^{-} = (x^2 - y^2 + 3)/7$$

$$u^{+} = 8, \quad u^{-} = \begin{cases} \sin(x + y) + \cos(x + y), & x + y \leqslant 0, \\ x + y + 1, & x + y > 0. \end{cases}$$

Note that the interface Γ is Lipschitz continuous but not C^1 and it has a kink at (0,0). The solution is C^1 but not C^2 on $\overline{\Omega^-}$ and the kink of the interface is on the non-C^2 of the solution. Fig. 18 shows the numerical solution using $\Omega^{5,5}$ of (4.8a) on the domain $(-1,3)\times(-1,1)$. Table 17 shows that the method achieves about 0.8th order accuracy in solutions on the whole domain. Varying orders of accuracy are observed under the grids (4.8c), since the singular point is not at relatively same locations in singular cells of the grids in the sequence (4.8c).

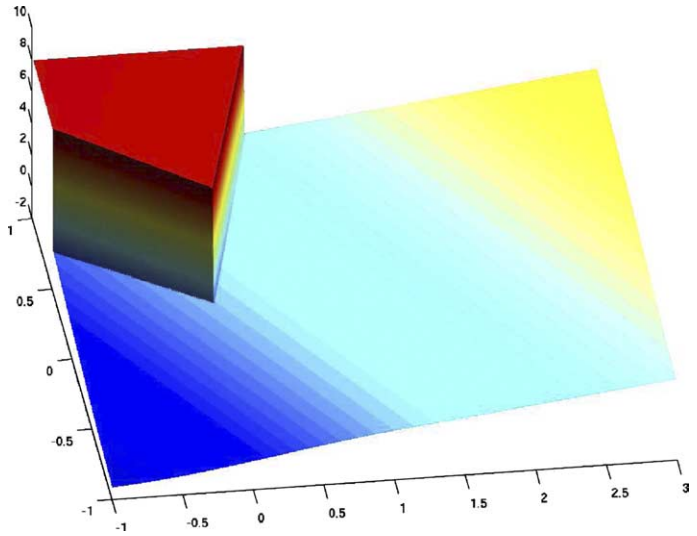

Fig. 18. Interface is Lipschitz continuous and has a kink at (0,0). The solution u is piecewise C^1. The kink (0,0) of the interface is on the non-C^2 points, $\{(x,-x)|x>0\}$, of the solution.

Table 17
About 0.8th order in u

Domain	# of pts in x, y	Err in u	Order	Err in ∇u
$(-1,3)\times(-1,1)$	41,21	3.35e−2		1.58e−1
	81,41	1.95e−2	0.78	1.38e−1
	161,81	1.11e−2	0.81	1.27e−1
	321,161	6.23e−3	0.83	1.21e−1
	641,321	3.45e−3	0.85	1.18e−1
$(-\frac{2\pi}{5},\frac{3\pi}{5})\times(-\frac{2\pi}{5},\frac{3\pi}{5})$	41,41	2.30e−2		1.31e−1
	81,81	1.32e−2	0.80	1.14e−1
	161,161	7.47e−3	0.82	1.05e−1
	321,321	4.17e−3	0.84	9.98e−2
$(-2,\frac{3\pi}{4})\times(-1,\frac{4\pi}{5})$	128, 128	7.02e−2		1.11e−0
	256, 256	4.20e−2	0.74	1.34e−0
	512, 512	8.82e−3	2.25	6.00e−1

Example 18. The level-set function ϕ, the coefficients $\beta^{\pm}$ and the solution $u^{\pm}$ are given as follows:

$$\phi = \begin{cases} y - 2x, & x + y > 0, \\ y + \frac{1}{2}x, & x + y \leqslant 0, \end{cases}$$
$$\beta^{+} = 1, \quad \beta^{-} = 2 + \sin(x + y),$$
$$u^{+} = 8, \quad u^{-} = (x^2 + y^2)^{\frac{5}{6}} + \sin(x + y).$$

Note that the interface Γ is only Lipschitz continuous and has a singular point at (0,0). Also the solution u is $H^2(\Omega^{\pm})$ and has a singular point (0,0), which coincides with the interface singular point. Fig. 19 shows the numerical solution of the method using $\Omega^{5,5}$ of (4.8a) on the domain $(-1,3) \times (-1,1)$. Table 18 shows

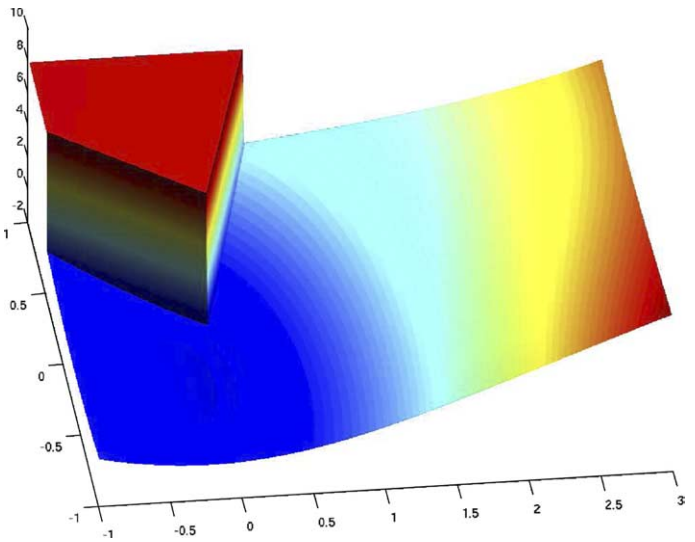

Fig. 19. Interface is Lipschitz continuous and has a kink at (0,0). u is piecewise H^2 and has a singular point at (0,0), which coincides with the interface singular point (0,0).

Table 18
About 0.8th order in u

Domain	# of pts in x, y	Err in u	Order	Err in ∇u
$(-1,3) \times (-1,1)$	41, 21	4.12e−2		1.42e−1
	81, 41	2.30e−2	0.84	1.25e−1
	161, 81	1.28e−2	0.85	1.15e−1
	321, 161	7.02e−3	0.86	1.08e−1
	641, 321	3.85e−3	0.87	1.04e−1
$(\frac{-2\pi}{5}, \frac{3\pi}{5}) \times (\frac{-2\pi}{5}, \frac{3\pi}{5})$	41, 41	3.02e−2		1.18e−1
	81, 81	1.66e−2	0.86	1.02e−1
	161, 161	9.04e−3	0.88	9.20e−2
	321, 321	4.92e−3	0.88	8.81e−2
$(-2, \frac{3\pi}{4}) \times (-1, \frac{4\pi}{5})$	128, 128	3.15e−2		1.83e−1
	256, 256	1.66e−2	0.92	1.74e−1
	512, 512	5.95e−4	4.80	8.87e−3

Table 19
Conclusion of numerical experiments

	Γ is C^2	Γ is C^1	Γ is Lipschitz continuous
$u(x,t)$ is C^2	2nd order in u and 1st order in ∇u	2nd order in u and 1st order in ∇u	0.8th order in u
$u(x,t)$ is C^1	1st order in u and 0.8th order in ∇u	1st order in u and 0.8th order in ∇u	0.8th order in u
$u(x,t)$ is H^2	1.6th order in u and 0.65th order in ∇u	1.6th order in u and 0.65th order in ∇u	0.8th order in u

that the method achieves about 0.8th order accuracy in solutions. Compared with the previous examples we observe that the kink of the interface, instead of the singularity of the solution, produces the dominant effect to bring down the order of accuracy. Varying orders of accuracy are observed under the grids (4.8c), since the singular point is not at relatively same locations in singular cells of the grids in the sequence (4.8c).

The conclusion of the numerical experiments are listed in the Table 19. Note that the result for the case in which the right hand side of the PDE blows up at a point is better than the result for a solution that is piecewise C^1, with bounded 2nd derivative. This is due to the fact that we have a straight line $\{(x,-x)|x < 0\}$ on which the latter solution is not C^2, while we only have one point (0,0) at which the former solution has unbounded 2nd derivative and at any other point the solution is C^∞.

5. Conclusion

In this work, a numerical method is developed to solve an elliptic problem in multi-dimensional space with variable coefficients, Lipschitz continuous interfaces and non-homogeneous interface conditions (2.1a)–(2.1c). A weak formulation (2.6a) and (2.6b) of the problem and its the existence, uniqueness and regularity of the weak solutions are studied, see Theorem 2.1. The method, Method 3.2, is derived from the weak formulation by a simple but new discretization, which is different from traditional finite element methods. The method uses non-body-fitting grids, hence irregular or uniform "triangulation" can be used. Methods using non-body-fitting grids have the advantage of avoiding costly grid regenerations over methods using body-fitting grids in the case when interfaces move. The method captures crispy sharp resolutions at interfaces. Extensive numerical experiments are presented and show that the method is 2nd order accurate in solution and 1st order accurate in its gradients in L^∞ norm if the interface is C^2 and solutions are C^2 on the closures of the subdomains. The method can handle the problems when the solutions and/or the interfaces are weaker than C^2. For example, $u \in H^2(\Omega^\pm)$, Γ is Lipschitz continuous and their singularities coincide, see Example 18 in Section 4. The accuracies of the method under various circumstances are listed in Table 19.

Acknowledgement

The authors thank Professor Gustavo Ponce, Professor Thomas Sideris and Professor Rugang Ye for their very helpful discussions.

Appendix A. Proof of Lemma 3.1

There are three typical cases for $U^h(u^h)$.

Case 0. If K is a regular triangle, see Fig. A.1. $U^h(u^h) = T^h(u^h)$, i.e.

$$U^h(u^h) = u(P_1) + \frac{u(P_2) - u(P_1)}{\Delta x}(x - x_i) + \frac{u(P_3) - u(P_1)}{\Delta y}(y - y_j). \tag{A.1}$$

Case 1. If K is an interface triangle, and the interface Γ cutting through two legs of K, see Fig. A.2, then

$$U^h(u^h) = \begin{cases} u(P_1) + u_x^+(x - x_i) + u_y^+(y - y_j), & (x,y) \in K^+, \\ u(P_2) + u_x^-(x - x_i - \Delta x) + (\frac{u(P_3) - u(P_2)}{\Delta y} + \frac{\Delta x}{\Delta y} u_x^-)(y - y_j), & (x,y) \in K^-. \end{cases} \tag{A.2}$$

Here $u_y^- = \frac{u(P_3) - u(P_2)}{\Delta y} + \frac{\Delta x}{\Delta y} u_x^-$. Three interface conditions are enforced as follows:

$$\begin{cases} \mathrm{d}x u_x^+ & +(\Delta x - \mathrm{d}x)u_x^- & & = r_1, \\ & (\Delta x - \frac{\Delta x}{\Delta y}\mathrm{d}y)u_x^- & +\mathrm{d}y u_y^+ & = r_2, \\ -\mathrm{d}y\beta^+ u_x^+ & +(\mathrm{d}y + \frac{\Delta x}{\Delta y}\mathrm{d}x)\beta^- u_x^- & -\mathrm{d}x\beta^+ u_y^+ & = r_3, \end{cases} \tag{A.3}$$

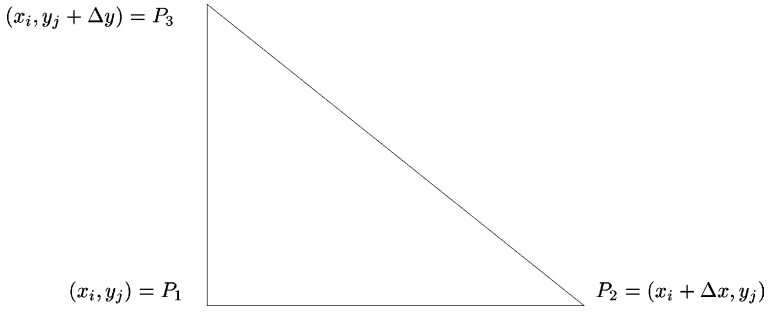

Fig. A.1. Case 0: the regular cell.

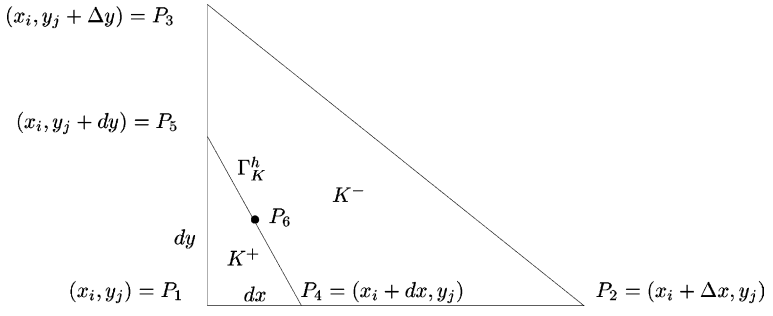

Fig. A.2. Case 1: the interface cutting through two legs of a triangle.

where $r_1 = u(P_2) - u(P_1) + a(P_4)$, $r_2 = u(P_2) - u(P_1) + \frac{u(P_3)-u(P_2)}{\Delta y}\mathrm{d}y + a(P_5)$, $r_3 = -\beta^- \frac{u(P_3)-u(P_2)}{\Delta y}\mathrm{d}x + b(P_6)\sqrt{\mathrm{d}x^2 + \mathrm{d}y^2}$. Here $\beta^+ = \frac{1}{|K^+|}\int_{K^+}\beta$ and $\beta^- = \frac{1}{|K^-|}\int_{K^-}\beta$ are the averages of β in K^+ and K^- regions (In the numerical experiments, we take β^+ to be the β at the center of K^+, and β^- the β at the center of K^-). Let

$$A = \begin{bmatrix} \mathrm{d}x & (\Delta x - \mathrm{d}x) & 0 \\ 0 & \Delta x - \frac{\Delta x}{\Delta y}\mathrm{d}y & \mathrm{d}y \\ -\mathrm{d}y\beta^+ & (\mathrm{d}y + \frac{\Delta x}{\Delta y}\mathrm{d}x)\beta^- & -\mathrm{d}x\beta^+ \end{bmatrix}, \quad A_1 = \begin{bmatrix} r_1 & (\Delta x - \mathrm{d}x) & 0 \\ r_2 & \Delta x - \frac{\Delta x}{\Delta y}\mathrm{d}y & \mathrm{d}y \\ r_3 & (\mathrm{d}y + \frac{\Delta x}{\Delta y}\mathrm{d}x)\beta^- & -\mathrm{d}x\beta^+ \end{bmatrix},$$
$$A_2 = \begin{bmatrix} \mathrm{d}x & r_1 & 0 \\ 0 & r_2 & \mathrm{d}y \\ -\mathrm{d}y\beta^+ & r_3 & -\mathrm{d}x\beta^+ \end{bmatrix}, \quad A_3 = \begin{bmatrix} \mathrm{d}x & (\Delta x - \mathrm{d}x) & r_1 \\ 0 & \Delta x - \frac{\Delta x}{\Delta y}\mathrm{d}y & r_2 \\ -\mathrm{d}y\beta^+ & (\mathrm{d}y + \frac{\Delta x}{\Delta y}\mathrm{d}x)\beta^- & r_3 \end{bmatrix}. \tag{A.4}$$

Clearly

$$\begin{aligned} u_x^+ &= \det(A_1)/\det(A), \quad u_x^- = \det(A_2)/\det(A), \\ u_y^+ &= \det(A_3)/\det(A), \quad u_y^- = \frac{u(P_3) - u(P_2)}{\Delta y} + \frac{\Delta x}{\Delta y}u_x^-. \end{aligned} \tag{A.5}$$

Note that the matrix A consists of information of grid, interface and coefficients β, and is independent from u^h, a or b. Also note that the determinants of matrices A_1, A_2 and A_3 are linear functions of u^h, a and b. Hence they could be rewritten in the forms of

$$\begin{aligned} u_x^+ &= c_{x,2}^+ \frac{u(P_2) - u(P_1)}{\Delta x} + c_{x,3}^+ \frac{u(P_3) - u(P_1)}{\Delta y} + c_{x,4}^+ a(P_4) + c_{x,5}^+ a(P_5) + c_{x,6}^+ b(P_6), \\ u_x^- &= c_{x,2}^- \frac{u(P_2) - u(P_1)}{\Delta x} + c_{x,3}^- \frac{u(P_3) - u(P_1)}{\Delta y} + c_{x,4}^- a(P_4) + c_{x,5}^- a(P_5) + c_{x,6}^- b(P_6), \\ u_y^+ &= c_{y,2}^+ \frac{u(P_2) - u(P_1)}{\Delta x} + c_{y,3}^+ \frac{u(P_3) - u(P_1)}{\Delta y} + c_{y,4}^+ a(P_4) + c_{y,5}^+ a(P_5) + c_{y,6}^+ b(P_6), \\ u_y^- &= c_{y,2}^- \frac{u(P_2) - u(P_1)}{\Delta x} + c_{y,3}^- \frac{u(P_3) - u(P_1)}{\Delta y} + c_{y,4}^- a(P_4) + c_{y,5}^- a(P_5) + c_{y,6}^- b(P_6). \end{aligned} \tag{A.6}$$

Lemma 6.1. *All coefficients c in (A.6) are finite and independent from u^h, a and b.*

Proof. From above discussion, it is easy to see that all coefficients c are independent from u^h, a and b. Below we prove that $c_{x,3}^+$ is finite. The proofs for the other coefficients are similar.

$$c_{x,3}^+ = \frac{-(\beta^+ - \beta^-)(\Delta x - \mathrm{d}x)\mathrm{d}x\,\mathrm{d}y}{\beta^+\left((\Delta x - \mathrm{d}x)\mathrm{d}y^2 + \frac{\Delta x}{\Delta y}(\Delta y - \mathrm{d}y)\mathrm{d}x^2\right) + \beta^-\left(\frac{\Delta x}{\Delta y}\,\mathrm{d}x^2\,\mathrm{d}y + \mathrm{d}y^2\,\mathrm{d}x\right)}. \tag{A.7}$$

It could be thought as a function of $\mathrm{d}x$ and $\mathrm{d}y$. It is smooth on $[0,\Delta x]\times[0,\Delta y]$ except one point $(\mathrm{d}x,\mathrm{d}y) = (0,0)$. It is easy to see that if $\mathrm{d}x = 0$ and $\mathrm{d}y \neq 0$, or $\mathrm{d}x \neq 0$ and $\mathrm{d}y = 0$, $c_{x,3}^+ = 0$. Now denote $k = \mathrm{d}y/\mathrm{d}x \in (0,+\infty)$, and rewrite it as

$$c_{x,3}^+ = \frac{-(\beta^+ - \beta^-)(\Delta x - \mathrm{d}x)k}{\beta^+\left((\Delta x - \mathrm{d}x)k^2 + \frac{\Delta x}{\Delta y}(\Delta y - k\,\mathrm{d}x)\right) + \beta^-\left(\frac{\Delta x}{\Delta y}\,\mathrm{d}xk + \mathrm{d}xk^2\right)}. \tag{A.8}$$

Let dx goes to zero,

$$\lim_{\mathrm{d}x\to 0,\ \mathrm{d}y=k\,\mathrm{d}x} c^{+}_{x,3} = \frac{-(\beta^{+}-\beta^{-})k}{\beta^{+}(k^2+1)}, \tag{A.9}$$

hence the limit is bounded for any $k \in (0,+\infty)$,

$$\lim_{\mathrm{d}x\to 0,\ \mathrm{d}y=k\,\mathrm{d}x} \mid c^{+}_{x,3} \mid \leqslant \left|\frac{-\beta^{+}+\beta^{-}}{\beta^{+}}\right|. \tag{A.10}$$

Therefore $\mid c^{+}_{x,3} \mid$ is bounded, for any $(\mathrm{d}x,\mathrm{d}y) \in [0,\Delta x]\times[0,\Delta y]$.

Case 2. If K is an interface triangle, and the interface Γ cutting through one leg and the hypotenuse of K, see Fig. A.3, then

$$U^h(u^h) = \begin{cases} u(P_2) + u^{+}_x(x-x_i-\Delta x) + u^{+}_y(y-y_j), & (x,y)\in K^{+}, \\ u(P_1) + u^{-}_x(x-x_i) + \frac{u(P_3)-u(P_1)}{\Delta y}(y-y_j), & (x,y)\in K^{-}. \end{cases} \tag{A.11}$$

Three interface conditions are enforced as follows:

$$\begin{cases} (-\mathrm{d}x)u^{+}_x & +(\mathrm{d}x-\Delta x)u^{-}_x & & = r_1, \\ -\frac{\Delta x}{\Delta y}\,\mathrm{d}y u^{+}_x & +(\frac{\Delta x}{\Delta y}\,\mathrm{d}y-\Delta x)u^{-}_x & +\mathrm{d}y u^{+}_y & = r_2, \\ \mathrm{d}y\beta^{+}u^{+}_x & -\mathrm{d}y\beta^{-}u^{-}_x & +(\frac{\Delta x}{\Delta y}\,\mathrm{d}y-\mathrm{d}x)\beta^{+}u^{+}_y & = r_3, \end{cases} \tag{A.12}$$

where $r_1 = u(P_1) - u(P_2) + a(P_4)$, $r_2 = u(P_1) - u(P_2) + \frac{u(P_3)-u(P_1)}{\Delta y}\,\mathrm{d}y + a(P_5)$, and $r_3 = \beta^{-}\frac{u(P_3)-u(P_1)}{\Delta y}(\frac{\Delta x}{\Delta y}\,\mathrm{d}y-\mathrm{d}x) + b(P_6)\sqrt{\mathrm{d}y^2+(\frac{\Delta x}{\Delta y}\,\mathrm{d}y-\mathrm{d}x)^2}$.

Let

$$A = \begin{bmatrix} -\mathrm{d}x & (\mathrm{d}x-\Delta x) & 0 \\ -\frac{\Delta x}{\Delta y}\,\mathrm{d}y & (\frac{\Delta x}{\Delta y}\,\mathrm{d}y-\Delta x) & \mathrm{d}y \\ \mathrm{d}y\beta^{+} & -\mathrm{d}y\beta^{-} & (\frac{\Delta x}{\Delta y}\mathrm{d}y-\mathrm{d}x)\beta^{+} \end{bmatrix}, \quad A_1 = \begin{bmatrix} r_1 & (\mathrm{d}x-\Delta x) & 0 \\ r_2 & (\frac{\Delta x}{\Delta y}\,\mathrm{d}y-\Delta x) & \mathrm{d}y \\ r_3 & -\mathrm{d}y\beta^{-} & (\frac{\Delta x}{\Delta y}\,\mathrm{d}y-\mathrm{d}x)\beta^{+} \end{bmatrix},$$

$$A_2 = \begin{bmatrix} -\mathrm{d}x & r_1 & 0 \\ -\frac{\Delta x}{\Delta y}\,\mathrm{d}y & r_2 & \mathrm{d}y \\ \mathrm{d}y\beta^{+} & r_3 & (\frac{\Delta x}{\Delta y}\,\mathrm{d}y-\mathrm{d}x)\beta^{+} \end{bmatrix}, \quad A_3 = \begin{bmatrix} -\mathrm{d}x & (\mathrm{d}x-\Delta x) & r_1 \\ -\frac{\Delta x}{\Delta y}\,\mathrm{d}y & (\frac{\Delta x}{\Delta y}\,\mathrm{d}y-\Delta x) & r_2 \\ \mathrm{d}y\beta^{+} & -\mathrm{d}y\beta^{-} & r_3 \end{bmatrix}. \tag{A.13}$$

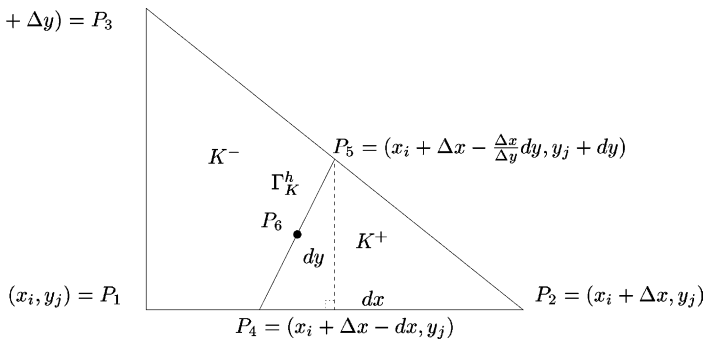

Fig. A.3. Case 2: the interface cutting through a leg and a hypotenuse of a triangle.

Clearly

$$u_x^+ = \det(A_1)/\det(A), \quad u_x^- = \det(A_2)/\det(A), \quad u_y^+ = \det(A_3)/\det(A), \quad u_y^- = \frac{u(P_3) - u(P_1)}{\Delta y}. \tag{A.14}$$

Same as in Case 1, the matrix A consists of information of grid, interface and coefficients β, and is independent from u^h, a or b. The determinants of matrices A_1, A_2 and A_3 are linear functions of u^h, a and b. Hence they could be rewritten in the forms of

$$\begin{aligned}
u_x^+ &= d_{x,2}^+ \frac{u(P_2) - u(P_1)}{\Delta x} + d_{x,3}^+ \frac{u(P_3) - u(P_1)}{\Delta y} + d_{x,4}^+ a(P_4) + d_{x,5}^+ a(P_5) + d_{x,6}^+ b(P_6),\\
u_x^- &= d_{x,2}^- \frac{u(P_2) - u(P_1)}{\Delta x} + d_{x,3}^- \frac{u(P_3) - u(P_1)}{\Delta y} + d_{x,4}^- a(P_4) + d_{x,5}^- a(P_5) + d_{x,6}^- b(P_6),\\
u_y^+ &= d_{y,2}^+ \frac{u(P_2) - u(P_1)}{\Delta x} + d_{y,3}^+ \frac{u(P_3) - u(P_1)}{\Delta y} + d_{y,4}^+ a(P_4) + d_{y,5}^+ a(P_5) + d_{y,6}^+ b(P_6),\\
u_y^- &= d_{y,2}^- \frac{u(P_2) - u(P_1)}{\Delta x} + d_{y,3}^- \frac{u(P_3) - u(P_1)}{\Delta y} + d_{y,4}^- a(P_4) + d_{y,5}^- a(P_5) + d_{y,6}^- b(P_6).
\end{aligned} \tag{A.15}$$

Lemma 6.2. *All coefficients d in (A.15) are finite and independent from u^h, a and b.*

Proof. The proof is the same as the proof of Lemma 6.1, and is omitted here.

From above discussion, we complete the proof of Lemma 6.1 and all coefficients c and d are independent from u^h, a and b.

References

[1] Chen Zhiming, Zou Jun, Finite element methods and their convergence for elliptic and parabolic interface problems, Numerische Mathematik 79 (1998) 175–202.
[2] R. Fedkiw, T. Aslam, B. Merriman, S. Osher, A non-oscillatory Eulerian approach to interfaces in multimaterial flows (The Ghost Fluid Method), J. Comput. Phys. 152 (2) (1999) 457–492.
[3] F. Gibou, R. Fedkiw, L.-T. Cheng, M.A. Kang, Second order accurate symmetric discretization of the poisson equation on irregular domains, J. Comput. Phys. 176 (2002) 1–23.
[4] P. Grisvard, Elliptic problems in nonsmooth domains – Monographs and Studies in Mathematics, Pitman Advanced Publishing Program. ISSN 0743-0329, 1985.
[5] R.J. LeVeque, Z. Li, The immersed interface method for elliptic equations with discontinuous coefficients and singular sources, SIAM J. Numer. Anal. 31 (1994) 1019.
[6] Z. Li, A fast iterative algorithm for elliptic interface problems, SIAM J. Numer. Anal. 35 (1) (1998) 230–254.
[7] Z. Li, T. Lin, X. Wu, New Cartesian grid methods for interface problems using the finite element formulation, Numerische Mathematik, 9661-98, (2003). Preprint. NCSU CRSC-TR99-12.
[8] Xu-Dong Liu, Ronald P. Fedkiw, Myungjoo Kang, A boundary condition capturing method for Poisson's equation on irregular domains, J. Comput. Phys. 160 (1) (2000) 151–178.
[9] X.-D. Liu, T. Sideris, Convergence of the Ghost fluid method for elliptic equations with interfaces, Math. Comp. 72 (2003).
[10] A. Mayo, The fast solution of poisson's and the biharmonic equations in irregular domains, SIAM J. Numer. Anal. 21 (2) (1984) 285–299.
[11] A. Mayo, Fast high order accurate solutions of laplace's equation on irregular domains, SIAM J. Sci. Stat. Comput. 6 (1) (1985) 144–157.

[12] J. Necas, Introduction to the theory of nonlinear elliptic equations, Teubner–Texte zur Mathematik. Band 52, ISSN 0138-502X, 1983.
[13] C. Peskin, Numerical analysis of blood flow in the heart, J. Comput. Phys. 25 (1977) 220–252.
[14] Peskin, C. and, B. Printz, Improved volume conservation in the computation of flows with immersed elastic boundaries, J. Comput. Phys. 105 (1993) 33–46.
[15] M. Sussman, P. Smereka, S. Osher, A level set approach for computing solutions to incompressible two-phase flow, J. Comput. Phys. 114 (1994) 146–154.
[16] Justin W.L. Wan, Xu-Dong Liu, A boundary condition capturing multigrid approach to irregular boundary problems, SIAM J. Sci. Comput. 25 (6) (2004) 1982–2003.